


Temporal and spatial frameworks supporting plant responses to vegetation proximity

Pedro Pastor-Andreu,¹  Jordi Moreno-Romero,^{1,2,3}  Mikel Urdin-Bravo,²  Julia Palau-Rodríguez,² Sandi Paulisic,¹ 
Elizabeth Kastanaki,⁴ Vicente Vives-Peris,⁵  Aurelio Gomez-Cadenas,⁵  Anna Esteve-Codina,⁶ Beatriz Martín-Mur,⁶
Antía Rodríguez-Villalón,⁴ Jaume F. Martínez-García^{1,2,*} 

¹Centre for Research in Agricultural Genomics (CRAG), CSIC-IRTA-UAB-UB, Barcelona 08193, Spain

²Institute for Plant Molecular and Cell Biology (IBMCP), CSIC-UPV, València 46022, Spain

³Departament de Bioquímica I Biologia Molecular, Universitat Autònoma de Barcelona, Barcelona 08193, Spain

⁴Group of Plant Vascular Development, Swiss Federal Institute of Technology (ETH) Zurich, Zurich CH-8092, Switzerland

⁵Departament de Biologia, Bioquímica I Ciències Naturals, Universitat Jaume I, Castelló de la Plana 12071, Spain

⁶Functional Genomics Team, Centro Nacional de Análisis Genómico (CNAG), Universitat de Barcelona, Barcelona 08028, Spain

*Author for correspondence: jaume.martinez@ibmcp.upv.es

The author responsible for distribution of materials integral to the findings presented in this article in accordance with the policy described in the Instructions for Authors (<https://academic.oup.com/plphys/pages/General-Instructions>) is: Jaume F. Martínez-García (jaume.martinez@ibmcp.upv.es).

Abstract

After the perception of vegetation proximity by phytochrome photoreceptors, shade-avoider plants initiate a set of responses known as the shade avoidance syndrome (SAS). Shade perception by the phytochrome B (phyB) photoreceptor unleashes the PHYTOCHROME INTERACTING FACTORS and initiates SAS responses. In *Arabidopsis* (*Arabidopsis thaliana*) seedlings, shade perception involves rapid and massive changes in gene expression, increases auxin production, and promotes hypocotyl elongation. Other components, such as phyA and ELONGATED HYPOCOTYL 5, also participate in the shade regulation of the hypocotyl elongation response by repressing it. However, why and how so many regulators with either positive or negative activities modulate the same response remains unclear. Our physiological, genetic, cellular, and transcriptomic analyses showed that (i) these components are organized into 2 main branches or modules and (ii) the connection between them is dynamic and changes with the time of shade exposure. We propose a model for the regulation of shade-induced hypocotyl elongation in which the temporal and spatial functional importance of the various SAS regulators analyzed here helps to explain the coexistence of differentiated regulatory branches with overlapping activities.

Introduction

When plants grow in high density, the close proximity of vegetation might obstruct sunlight and pose a threat for plant survival. Plants have adopted contrasting avoidance or tolerance strategies to deal with vegetation proximity or shade (Martínez-García and Rodríguez-Concepcion 2023). Specifically, when shade-avoider (sun-loving) plants face this scenario, they display a set of responses known as the shade avoidance syndrome (SAS). Some of the SAS responses acclimate photosynthesis to eventual light shortage caused by the presence of neighboring plants; others focus on redirecting growth to escape from shade by promoting either stem elongation and/or apical dominance (reduced branching) or flowering to produce seeds (Casal 2012; Roig-Villanova and Martínez-García 2016; Morelli et al. 2021). At the seedling stage, hypocotyl elongation is likely the best characterized and most conspicuous SAS response in the shade-avoider plant *Arabidopsis* (*Arabidopsis thaliana*) (Casal 2012; Martínez-García et al. 2014) and the focus of this work.

Plants detect neighbor vegetation as changes in the red (R) to far-red light (FR) ratio (R:FR). Plants absorb R and reflect mainly FR from sunlight. Under low planting density, the intensity of incoming sunlight during the day changes but the R:FR (>1.2)

remains relatively constant (Smith 1982). By contrast, when neighboring plants are close enough, they can sense plant proximity by detecting the reflected FR from other plants that combines with sunlight and results in a moderate decrease in the R:FR (R:FR 0.5 to 0.3) without reducing light intensity. When neighboring vegetation is denser forming a plant canopy, photosynthetic pigments of the upper leaves act as selective filters that preferentially absorb and deplete blue and R from sunlight but transmit part of green and most FR (Casal 2012). Plant canopy shade presents a drastic reduction of R compared to the FR that results in a very low R:FR ratio (R:FR < 0.06) and a low light intensity in the photosynthetic active radiation region (Martínez-García et al. 2014; Pierik and de Wit 2014; Fiorucci and Fankhauser 2017). The reduced R:FR occurring under both proximity and canopy shade acts as a reliable signal indicative of the nearby presence of vegetation that is perceived by the phytochrome photoreceptors (Fig. 1).

As molecular switches, phytochromes exist in 2 photoconvertible isoforms (an inactive R-absorbing Pr form and an active FR-absorbing Pfr form) that are present in an equilibrium that depends on the prevailing R:FR. Under high R:FR (low vegetation density), most phytochromes are in the active Pfr forms and SAS

Received October 17, 2023. Accepted July 7, 2024.

© The Author(s) 2024. Published by Oxford University Press on behalf of American Society of Plant Biologists.

This is an Open Access article distributed under the terms of the Creative Commons Attribution-NonCommercial-NoDerivs licence (<https://creativecommons.org/licenses/by-nc-nd/4.0/>), which permits non-commercial reproduction and distribution of the work, in any medium, provided the original work is not altered or transformed in any way, and that the work is properly cited. For commercial re-use, please contact reprints@oup.com for reprints and translation rights for reprints. All other permissions can be obtained through our RightsLink service via the Permissions link on the article page on our site—for further information please contact journals.permissions@oup.com.

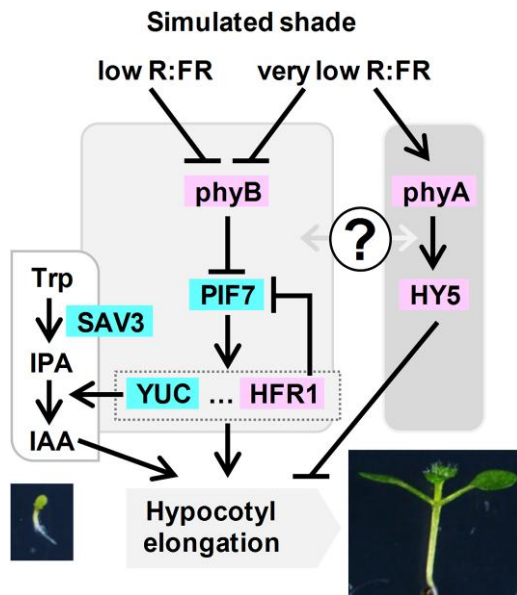


Figure 1. Simplified model that depicts the genetic components analyzed in this work involved in plant neighbor detection. Color indicates the positive (blue) or negative (pink) contribution to the shade-induced hypocotyl elongation. Aspect of representative seedlings just before (W-grown 2-d-old, bottom left) and after the shade treatment (shade-grown 7-d-old, bottom right) is shown. Arrows indicate positive and bars represent negative regulatory relationships. Question mark indicates an unknown regulatory relationship between the connected components.

is suppressed, whereas under low R:FR (high vegetation density), the photoequilibrium moves toward the inactive Pr form and SAS is induced. From the 5 phytochromes characterized in *A. thaliana* (phytochrome A [phyA] to phyE), phyA and phyB have the main roles in controlling SAS responses. Genetic and physiological analyses indicate that photostable phyB is the major phytochrome controlling the SAS (Casal 2012; Martínez-García et al. 2014). Additional genetic analyses also showed that phyA, the only photolabile phytochrome, has an antagonistic role over phyB in the SAS control, particularly under very low R:FR mimicking plant canopy shade. Under low R:FR (proximity shade), wild-type and *phyA* mutant seedlings present a similar hypocotyl elongation whereas *phyB* mutants display longer hypocotyls. In contrast, under very low R:FR (canopy shade), wild-type and *phyB* seedlings elongate less than when grown under low R:FR and *phyA* seedlings present an exaggerated hypocotyl length. This indicates that phyB is deactivated by both proximity (low R:FR) and canopy (very low R:FR) shade whereas phyA activity is induced only by very low R:FR (Fig. 1) (Yanovsky et al. 1995; Martínez-García et al. 2014; Molina-Contreras et al. 2019). It has been shown that under very low R:FR conditions, phyA protein tends to accumulate (Martínez-García et al. 2014; Yang et al. 2018; Molina-Contreras et al. 2019). For clarity, we will use the term simulated shade to refer to any treatment, including proximity, canopy, or other similar conditions, that lowers the R:FR but has not been specifically defined as such (Roig-Villanova and Martínez-García 2022).

SAS implementation is regulated by, at least, the interaction of active phyB with PHYTOCHROME INTERACTING FACTORS (PIFs), a family of basic-helix-loop-helix (bHLH) transcription factors. When interacting with active phyB, PIFs are phosphorylated. Phosphorylation triggers the degradation of PIF1, PIF3, PIF4, and PIF5 (known as the PIF quartet [PIFQ]) via the 26S proteasome. By contrast, PIF7 phosphorylation has little effect on its stability but

it inhibits its DNA-binding activity (Li et al. 2012) and promotes cytoplasm retention, reducing its nuclear import (Huang et al. 2018). Either case, under high R:FR, PIF transcriptional activity is inhibited by the active form of phyB, whereas deactivation of phyB under low R:FR results in PIF accumulation in the nucleus and/or promotion of their DNA-binding activity. This initiates a transcriptional cascade that leads to the expression of dozens of PHYTOCHROME RAPIDLY REGULATED (PAR) genes, several of which encode transcription factors from various families (e.g. bHLH, HD-Zip, and BBX) having positive, negative, or even complex roles in implementing the hypocotyl elongation response (Sessa et al. 2005; Roig-Villanova et al. 2006, 2007; Sorin et al. 2009; Cifuentes-Esquivel et al. 2013; Ciolfi et al. 2013; Gangappa et al. 2013; Kohnen et al. 2016; Gallemi et al. 2017; Gommers et al. 2017; Buti et al. 2020).

PIF7, together with a minor contribution of PIF4 and PIF5, has a major and positive role in promoting the shade-induced hypocotyl elongation. *pif7* and the *pif4 pif5 pif7* (from now on *pif457*) showed an attenuated and almost null hypocotyl elongation in response to simulated shade (Li et al. 2012; de Wit et al. 2015). From the various PAR genes, induction of YUCCAs (YUCs) contributes to auxin production together with SHADE AVOIDANCE 3 (SAV3, also known as TRYPTOPHAN AMINOTRANSFERASE OF ARABIDOPSIS 1/WEAK ETHYLENE INSENSITIVE 8 [TAA1/WEI8]) in the 2-step indole-3-acetic acid (IAA) pathway from tryptophan (Trp). Indeed, the Trp aminotransferase encoded by SAV3 catalyzes the conversion from Trp to indole-3-pyruvic acid (IPA), and the flavin monooxygenase encoded by YUC genes catalyzes the IPA oxidative decarboxylation to IAA (Fig. 1) (Brumos et al. 2014; Zheng et al. 2016). The single *sav3* and multiple mutants in YUC genes (*yuc2 yuc5 yuc8 yuc9* and *yuc3 yuc5 yuc7 yuc8 yuc9*) had attenuated shade-induced hypocotyl elongation (Li et al. 2012; Kohnen et al. 2016). Together, these results highlight the importance of SAV3- and YUC-mediated production of IAA in this SAS response.

Another PAR gene with a well-known negative role in the shade-induced hypocotyl elongation is LONG HYPOCOTYL IN FAR-RED 1 (HFR1) that encodes a transcriptional cofactor of the bHLH family structurally related to PIFs but lacks the phyB- and DNA-binding ability (Galstyan et al. 2011; Hornitschek et al. 2012). HFR1 heterodimerizes and inhibits the activity of all 4 PIFQ members (PIF1, PIF3, PIF4, and PIF5) (Fairchild et al. 2000; Hornitschek et al. 2009; Shi et al. 2013) and PIF7 (Zhang et al. 2019; Buti et al. 2020; Paulisic et al. 2021). *hfr1* hypocotyls display an opposed phenotype to that of *pif7* or *pif457* seedlings; i.e. they are longer than wild-type ones under simulated shade (Roig-Villanova et al. 2007; Ciolfi et al. 2013; de Wit et al. 2016). Another PIF antagonist is ELONGATED HYPOCOTYL 5 (HY5), known to encode a transcription factor of the basic domain-leucine zipper (bZIP) family. HY5 expression is phyA-dependent, and it is not rapidly or strongly induced in response to certain shade condition (Ciolfi et al. 2013). Hypocotyls of the *hy5* mutant seedlings elongate more than the wild-type ones under low R:FR (Sellaro et al. 2011; Bou-Torrent et al. 2015; van Gelderen et al. 2018; Ortiz-Alcaide et al. 2019). Therefore, HY5 acts as a negative SAS regulator. CONSTITUTIVELY PHOTOMORPHOGENIC 1 (COP1) is an E3 ubiquitin ligase that interacts with and modulates the abundance of several SAS regulatory components, including HY5 and HFR1. COP1 accumulates in the nucleus under shade, counteracting the negative impact of HY5 and HFR1 accumulation and modulating therefore this response (Pacín et al. 2013, 2016). Nuclear-pore complex components, chloroplast-derived signals, and epigenetic components also prevent an excessive response to shade, providing additional levels of regulation of this response (Gallemi et al. 2016; Ortiz-Alcaide et al. 2019; Martínez-García and Moreno-Romero 2020).

The mechanisms that connect SAS components have been established in a few cases: (i) HFR1 inhibits PIF activity; (ii) HY5 appears to be mainly associated with phyA action (Ciolfi et al. 2013; Zhang et al. 2018), although it has not been explored; and (iii) other transcription factors, including the growth-promoting PIFs, would be mostly linked to the phyB-dependent pathway (Casal 2012; Roig-Villanova and Martínez-García 2016) (Fig. 1). The antagonistic phyA/HY5/HFR1 and phyB/PIF/SAV3 activities likely provide young seedlings with the capacity to rapidly elongate when impeding competition is nearby and also to attenuate excessive growth when growing under a canopy. However, several key aspects of the genetic architecture of the SAS regulatory network remain unclear. These include features regarding whether these pathways or components operate concurrently on the same cell type and, if they do, how they are connected (Fig. 1). To address these issues, we have carried out (i) genetic analyses, to establish if different SAS components work in the same or different regulatory branches or modules of the network; (ii) temporal analyses, to learn when the different components analyzed act in controlling the shade-induced hypocotyl elongation; and (iii) spatial analyses, to identify the cells targeted along the hypocotyl axis epidermis by each SAS regulator. Besides, we explored molecular connections between HY5 and PIFs, 2 antagonistic SAS components. Our findings indicated that these components are grouped in, at least, 2 main modules or branches that act at different times and impact the elongation of distinct cells along the hypocotyl axis. We also show that HY5 acts as a node, although its functional relationship with PIF457 changes with the time of shade exposure.

Results

The SAS regulatory network is organized in at least 2 genetically differentiated modules or branches

We first prepared a series of genetic crosses focusing on a few mutants in negative (*phyA*, *phyB*, *HY5*, and *HFR1*) or positive (*SAV3*, *PIF4*, *PIF5*, and *PIF7*) SAS components (Fig. 1). These mutants result in strong shade-related hypocotyl phenotypes. From these components, only *PIF4*, *PIF5*, and *PIF7* (*PIF457*) show some redundancy in controlling the shade-induced hypocotyl elongation (Li et al. 2012; Hersch et al. 2014).

The hypocotyl length of the single and double *phyA* and *phyB* mutant seedlings in response to simulated shade was first analyzed (Fig. 2). In continuous white light (W) (that simulates sunlight of high R:FR), the length of *Col-0* and *phyA* hypocotyls was similar, whereas that of *phyB* hypocotyls was longer and those of *phyA phyB* double mutant seedlings were the longest, as expected. In continuous W + FR (very low R:FR), *phyA* hypocotyls were longer and *phyB* hypocotyls shorter, respectively, than the wild type (Fig. 2, A and B). The antagonistic activity of *phyA* and *phyB* under simulated shade indicates that the W + FR conditions employed in these experiments mimic canopy shade, in contrast with those proximity shade conditions in which *phyA* action is negligible (Martínez-García et al. 2014). Importantly, the *phyA phyB* hypocotyl length in W + FR was even longer than in W (Fig. 2B), in agreement with the conclusion that other phytochromes regulate the shade-induced hypocotyl elongation (Devlin et al. 2003). To better visualize the effect of simulated shade in controlling hypocotyl elongation, the difference in hypocotyl length in W + FR and W ($HYP_{W+FR} - HYP_W$) was calculated (Fig. 2C). This representation showed that *phyA phyB* double mutant hypocotyls had an

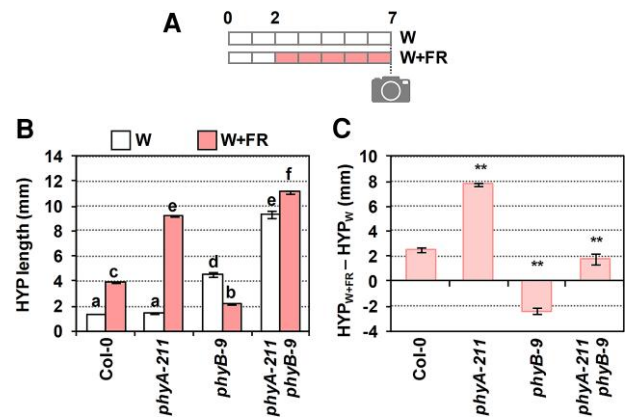


Figure 2. Genetic interaction of *phyA* and *phyB* in the shade-induced hypocotyl elongation. **A)** Cartoon showing the design of the experiment. Seedlings were germinated and grown in W (R:FR > 1.5) for 2 d, and then they either maintained in W or transferred to simulated shade (W + FR, R:FR, 0.02) for 5 more days. On Day 7, pictures were taken and hypocotyl (*HYP*) length was measured. **B)** *HYP* length of *Col-0*, *phyA-211*, *phyB-9*, and *phyA-211 phyB-9* double mutant seedlings after growing in W (HYP_W) or W + FR (HYP_{W+FR}). Values are means and error bars are SE of 3 independent replicates. **C)** Elongation response ($HYP_{W+FR} - HYP_W$) of lines shown in **B)**. Values of HYP_W and HYP_{W+FR} (shown in **B)** were used to calculate $HYP_{W+FR} - HYP_W$. SE was propagated accordingly. In **B)**, different letters denote significant differences (2-way ANOVA with the Tukey test, $P < 0.05$) among means. In **C)**, asterisks indicate significant differences (based on the 2-way ANOVA) between the mutant and wild-type genotypes in response to simulated shade (** $P < 0.01$).

intermediate shade-induced elongation response compared to those of *phyA* and *phyB* single mutants (Fig. 2C), suggesting that the effect of the 2 phytochromes is additive. This is interpreted as indicative that these 2 phytochromes act likely independently of one another in controlling the shade-induced hypocotyl length. In the following set of experiments, the $HYP_{W+FR} - HYP_W$ is shown when comparing the different mutants (raw data are included as Supplementary data).

We next produced double mutants deficient in other negative regulators (*phyA hfr1*, *hy5 hfr1*, and *phyA hy5*) and analyzed their shade-induced hypocotyl elongation response (Fig. 3; Supplementary Fig. S1) (no *phyB* mutant was included in these crosses as its phenotype was observed more clearly in W). Seedlings of *phyA hfr1* and *hy5 hfr1* double mutants elongated more than the single mutants (Fig. 3, A and B), suggesting that they worked additively, in agreement with previous information (Kim et al. 2002; Ciolfi et al. 2013). By contrast, *phyA hy5* seedlings elongated as much as the *phyA* single mutant (Fig. 3C), indicating that *phyA* was epistatic over *HY5*. During deetiolation under monochromatic FR, hundreds of *phyA*-associated genes that are *phyA* regulated have been identified as putative direct targets of *phyA*. These direct targets are likely to be cotargeted by *phyA* in association with many known light-related transcription factors, such as *HY5* (Chen et al. 2014). It is therefore expected that several other DNA-binding or light-related transcription factors act downstream *phyA*. Following this model, epistasis reflects the upstream activity of *phyA* over *HY5* under our very low R:FR conditions, and it also involves the additional action of other factors (e.g. *HYH*). Together, our genetic analyses suggested that (i) *phyA* and *HY5* act in the same branch of the SAS regulatory network and that (ii) *HFR1* acts independently of *phyA* and *HY5* in controlling this response.

We also generated multiple mutants of positive and negative SAS regulators (Fig. 4; Supplementary Fig. S2). As before, *phyB* mutants were excluded from these crosses. Phenotypic analyses

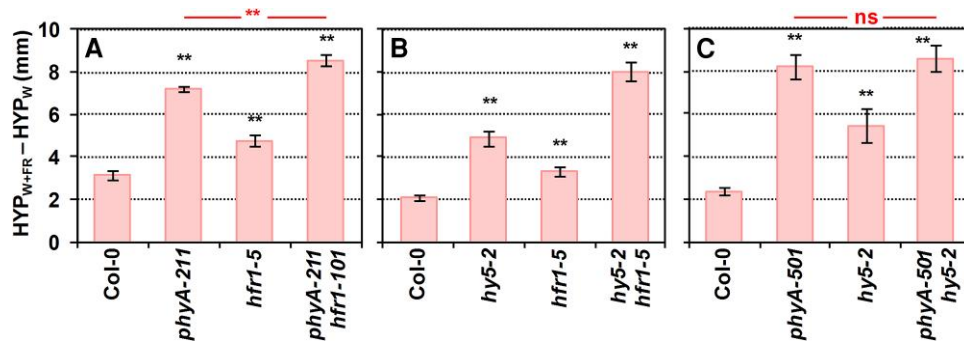


Figure 3. Genetic interaction of SAS-negative regulators in the shade-induced hypocotyl elongation. Difference of hypocotyl length (HYP) in simulated shade, W + FR (HYP_{W+FR}) and W (HYP_W) of Col-0, **A**) *phyA-211*, *hfr1-5*, *phyA-211 hfr1-101*, **B**) *hy5-2*, *hfr1-5*, *hy5-2 hfr1-1*, **C**) *phyA-501*, *hy5-2*, and *phyA-501 hy5-2*. Seedlings were grown as in Fig. 2A. Means and SE of 3 independent replicates were used to calculate the shown values of $HYP_{W+FR} - HYP_W$ and to propagate the SE . Error bars are the propagated SE . Black asterisks indicate significant differences (based on the 2-way ANOVA) between the mutant and wild-type genotypes in response to simulated shade (** $P < 0.01$). In **A**) and **C**), red asterisks indicate significant differences (based on the 2-way ANOVA) between the double mutants and *phyA* single genotypes in response to simulated shade (** $P < 0.01$; ns, not significant).

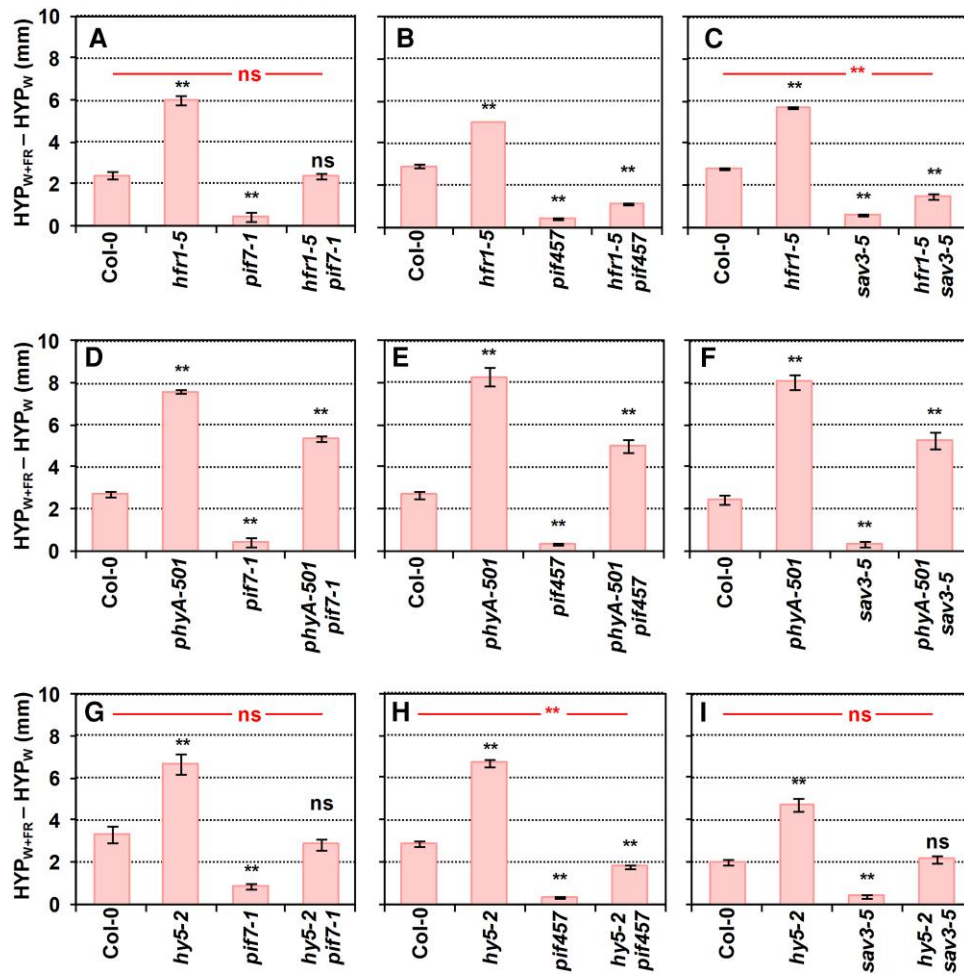


Figure 4. Genetic interaction of pairs of SAS-negative and -positive regulators in the shade-induced hypocotyl elongation. Difference of hypocotyl length (HYP) in simulated shade, W + FR (HYP_{W+FR}) and W (HYP_W) of Col-0 **A**) *hfr1-5*, *pif7-1*, *hfr1-5 pif7-1*, **B**) *hfr1-5*, *pif457*, *hfr1-5 pif457*, **C**) *hfr1-5*, *sav3-5*, *hfr1-5 sav3-5*, **D**) *phyA-501*, *pif7-1*, *phyA-501 pif7-1*, **E**) *phyA-501*, *pif457*, *phyA-501 pif457*, **F**) *phyA-501*, *sav3-5*, *phyA-501 sav3-5*, **G**) *hy5-2*, *pif7-1*, *hy5-2 pif7-1*, **H**) *hy5-2*, *pif457*, *hy5-2 pif457*, and **I**) *hy5-2*, *sav3-5*, and *hy5-2 sav3-5*. Seedlings were grown as in Fig. 2A. Means and SE of 3 independent replicates were used to calculate the shown values of $HYP_{W+FR} - HYP_W$ and to propagate the SE . Error bars are the propagated SE . Asterisks indicate significant differences (based on the 2-way ANOVA) between the mutant and wild-type genotypes in response to simulated shade (** $P < 0.01$; ns, not significant).

showed that *hfr1 pif7* length was intermediate between the single mutants (Fig. 4A; Supplementary Fig. S2A) consistent with HFR1 interacting with and inhibiting PIF7 activity (Fiorucci and

Fankhauser 2017; Buti et al. 2020; Paulisic et al. 2021). The shade-induced elongation of hypocotyls of an *hfr1 pif457* quadruple mutant line was reduced compared to *hfr1 pif7*. This is

consistent with the reported role of HFR1 as a transcriptional cofactor by heterodimerizing and inhibiting the transcriptional activity of PIF4 and PIF5 (Hornitschek et al. 2009; Galstyan et al. 2011). However, the elongation response of the *hfr1 pif457* mutant was still higher than that of *pif457* seedlings (Fig. 4B; Supplementary Fig. S2B), reflecting the minor contribution of additional factors. Mutant *hfr1* plants were also crossed with *sav3*, known to have a role in the shade-induced auxin biosynthesis (Tao et al. 2008). Phenotypic analyses (Fig. 4C; Supplementary Fig. S2C) showed that the phenotype of *hfr1 sav3* mutants was significantly longer than in *sav3* seedlings and virtually as short as *hfr1 pif457*, in agreement with the described role of PIF457 in promoting the SAV3-dependent IAA biosynthesis (Hornitschek et al. 2012; Li et al. 2012). These results not only pointed to a very minor contribution of other PIFs but also to a SAV3-independent auxin mechanism in these shade conditions.

In contrast with the previous crosses, *phyA pif7*, *phyA pif457*, and *phyA sav3* shade-induced hypocotyl elongation was similar between them and closer in length to that of *phyA* than to *pif7*, *pif457*, or *sav3* (Fig. 4, D to F; Supplementary Fig. S2, D to F). Together, these results suggested that the elongation repression imposed by *phyA* under simulated shade is mostly independent on PIF457 or the rapid shade-induced and SAV3-dependent auxin biosynthesis. Finally, hypocotyls of *hy5 pif7*, *hy5 pif457*, and *hy5 sav3* seedlings showed an intermediate elongation compared to the parental *pif7*, *pif457*, *sav3*, and *hy5* lines (Fig. 4, G to I; Supplementary Fig. S2, G to I). Together, these results suggest an additive activity for these regulators in the control of this shade-induced elongation response.

The variations in SAV3 requirements between the 2 proposed branches led us to explore the contribution of auxin synthesis and transport in these modules. The cotyledons of *A. thaliana* and *Brassica rapa* seedlings perceive shade and trigger local IAA synthesis in the cotyledons themselves (Fig. 1). Then, IAA is transported from cotyledons to the hypocotyl, where cellular elongation occurs (Procko et al. 2014). Treatments of wild-type seedlings with the auxin biosynthesis inhibitor L-kynurenine (L-kyn) that effectively and specifically targets Trp aminotransferases such as SAV3 (He et al. 2011) or with the auxin transport inhibitor naphthylphthalamic acid (NPA) abolish the shade-induced hypocotyl elongation response in wild-type seedlings (Fig. 5) (Sorin et al. 2009; Keuskamp et al. 2010; Hersch et al. 2014; Zheng et al. 2016). In our W + FR conditions, the extra elongation of *hfr1* compared to wild-type hypocotyls was completely abolished by the highest doses of L-kyn applied (Fig. 5A). Auxin quantification indicated that IAA levels in Col-0 and *hfr1* seedlings increased to similar values after 1 h of W + FR treatment (Fig. 5B), in contrast with published information (Hersch et al. 2014). Nonetheless, this result suggests that HFR1 does not have a strong and measurable impact on the IAA levels in our growth/shade conditions, at least at the time of shade treatment analyzed. The extra hypocotyl elongation of *phyA* and *hy5* seedlings, which was less affected by L-kyn than the wild type (Fig. 5A), and the attenuated IAA levels after 1 h of W + FR in both *hy5* and *phyA* (Fig. 5B) suggested that shade-induced elongation in these 2 mutants was not fully dependent on auxin levels. As IAA levels seem to be under negative feedback control, as in several auxin-signaling mutants (Suzuki et al. 2015; Takato et al. 2017), these results are consistent with *phyA* and *hy5* having an altered auxin responsiveness (Cluis et al. 2004; Yang et al. 2018).

The extra elongation of *hfr1* mutant seedlings is almost abolished by the application of the auxin transport inhibitor NPA (Fig. 5C), which indicates that the action of PIF-HFR1 in modulating the shade-induced hypocotyl elongation is mostly dependent on auxin produced somewhere else and transported to the hypocotyl, as

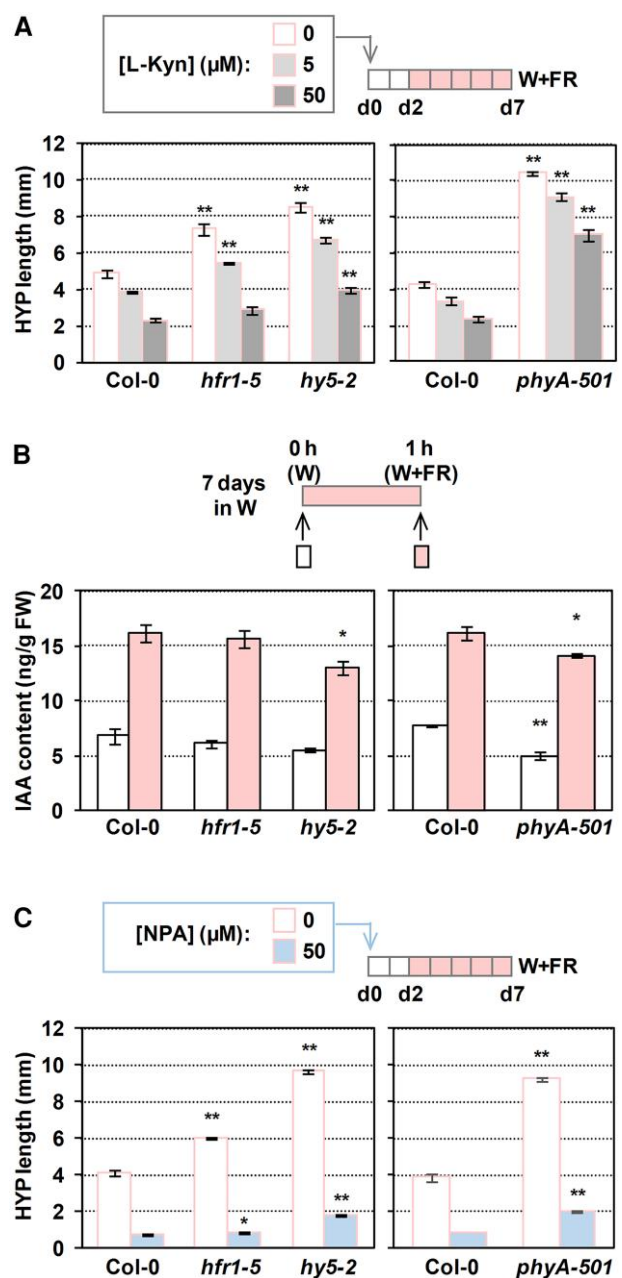


Figure 5. Contribution of auxin synthesis and polar transport in the shade-induced hypocotyl response of *phyA*, *hy5*, and *hfr1* seedlings. **A)** Effect of L-kyn on the shade-induced hypocotyl (HYP) length of Col-0, *hfr1-5*, *hy5-2*, and *phyA-501* seedlings. **B)** IAA content in Col-0, *hfr1-5*, *hy5-2*, and *phyA-501* seedlings grown in W for 7 d and then treated for 1 h with W + FR (R:FR = 0.02). Whole seedlings were collected to measure IAA levels. Data are means and error bars are SE of 4 biological replicates. FW, fresh weight. **C)** Effect of NPA on the shade-induced HYP length of Col-0, *hfr1-5*, *hy5-2*, and *phyA-501* seedlings. In **A)** and **C)**, inhibitors were applied in the media, seedlings were grown in W for 2 d and then transferred to W + FR for 5 d, and values are means and error bars are SE of 3 independent replicates. Asterisks indicate significant differences (Student's t-test) relative to the wild type growing under the same light treatment (ns, not significant, * $P < 0.05$, ** $P < 0.01$).

proposed (Hersch et al. 2014). By contrast, the resistance to the inhibitory effect of NPA of *phyA* and *hy5* (Fig. 5C) suggested that these 2 factors share similar mechanisms to repress shade-induced elongation and, in contrast with HFR1, are less dependent on auxin transport to promote elongation.

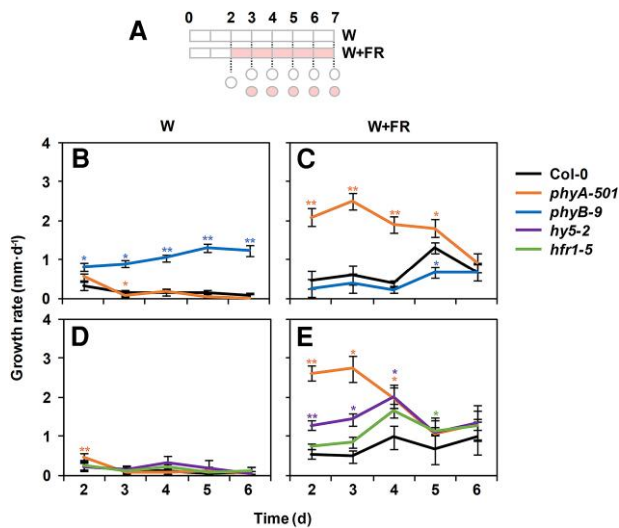


Figure 6. Effect of *phyA*, *phyB*, *HFR1*, and *HY5* mutations on the hypocotyl growth rate under W and simulated shade. **A)** Cartoon of the experiment design. Seeds were germinated and grown for 2 d under W and then either kept under W or transferred to simulated shade (W + FR, R:FR=0.02) for 5 more days. Circles indicate the days on which hypocotyl lengths were measured to estimate the daily growth rate. Growth rate of Col-0, *phyA-501*, and *phyB-9* hypocotyls grown in W **B)** or W + FR **C)**. Growth rate of Col-0, *phyA-501*, *hfr1-5*, and *hy5-2* hypocotyls grown in W **D)** or W + FR **E)**. In **B)** to **E)**, growth rate values were estimated as the difference of average hypocotyl length after 2 consecutive days. Values are means and error bars are SE of 3 independent biological replicates.

Together, these results are consistent with a network architecture in which these components are likely organized in at least 2 separate branches or modules, one involving the activity of PIF457, *HFR1*, and *SAV3* to promote the shade-induced hypocotyl elongation and a second one requiring the activity of *PHYA* and *HY5* to repress it.

SAS regulatory components act in different moments during the shade-induced hypocotyl elongation

We next studied when the different components act upon exposure of young seedlings to W + FR. Growth rates were first determined in wild-type (Col-0) seedlings grown under W and W + FR. To do so, hypocotyl length was measured daily from Days 2 to 7 in different groups of seedlings, and the variations in the daily growth rate were estimated for each genotype and light treatment (Fig. 6A). Under W, Col-0 growth rate remained low but constant along the period analyzed (Fig. 6, B and D), whereas under W + FR, it went up from Day 5 onwards (Fig. 6, C and E). As an additional control, the growth rate of the *phyB* mutant hypocotyls was also estimated. Importantly, under W, *phyB* growth rate increased with the age of the seedlings (Fig. 6B). Under W + FR, *phyB* growth rate mimicked that of Col-0 but the peak at Day 5 was attenuated in the mutant (Fig. 6C), consistent with its reduced elongation compared to Col-0 (Fig. 2) (Martínez-García et al. 2014; Molina-Contreras et al. 2019). Under W, the growth rate of *phyA*, *hy5*, and *hfr1* hypocotyls was constant along time and similar to that of Col-0 (Fig. 6, B and D). Under W + FR, *phyA* and, to a lower extent, *hy5* growth rate was much higher than that of Col-0 hypocotyls on Days 2 to 4 but progressively dropped to values closer to those of Col-0 (Fig. 6, C and E). By contrast, *hfr1* followed a pattern of growth rate similar to Col-0 and, if anything, it elongated slightly faster than Col-0 in the second half

of the period of time analyzed (Fig. 6E). To visualize the repressor activity of the different regulators, the growth rate of the wild type was subtracted to that of each mutant grown in those conditions where the phenotype is more obvious: W for *phyB* and W + FR for *hfr1*, *hy5*, and *phyA*. This representation confirmed our previous conclusions (Supplementary Fig. S3). In summary, although the temporal activity of the regulators overlapped, *phyA* represses hypocotyl elongation more strongly at the beginning of seedling development (from Days 2 to 4), *HY5* at the beginning but shows a peak in the middle of this period (Day 4) and *HFR1* (and *phyB*) appeared as more active at the second half of the period analyzed (from Days 5 to 7). These results provided a framework that separates the temporal action of the participating components.

SAS regulatory components target overlapping but different regions along the hypocotyl axis

In *A. thaliana*, hypocotyl elongation is a result of cell elongation (not cell division). Among the different tissues of this organ, the epidermis is of particular importance in mediating auxin-induced growth in the hypocotyl (Procko et al. 2016). In W-grown hypocotyls, the pattern of epidermal cell length takes place in all cells over the entire growth period (from 1 to 9 d after germination), although the area of fastest growth moves acropetally, from the base (Cells 2 to 4) on Days 1 to 2 to the middle (Cells 10 to 12) of the hypocotyl on Days 7 to 9 (Gendreau et al. 1997). In dark-grown seedlings, growth also initiates in the hypocotyl basal cells but, in this case, cells that elongated fastest move up much more rapidly and only a few cells upwards: from Cell 1 at 36 to 48 h to Cells 3 to 4 at 72 h from germination (Gendreau et al. 1997). As there is not much information about how *A. thaliana* hypocotyls elongate in response to simulated shade at the cell level, we first established the pattern of epidermal cell length in wild-type (Col-0) hypocotyls grown under W and W + FR. Using confocal microscopy, the length of several files of epidermal cells along the hypocotyl longitudinal axis per treatment was measured (Supplementary Fig. S4). Cell length in W-grown hypocotyls was similar along the hypocotyl (Supplementary Fig. S5). By contrast, W + FR treatment enhanced the elongation of all cells compared to W treatment, although the pattern of epidermal cell length was not uniformly distributed, with cells located in the lower half of the hypocotyl elongating the most (Supplementary Fig. S5). A similar conclusion was reached when representing the difference in length between cells grown in W + FR and W in each position, with Cells 7 to 8 being the ones that grew the most, becoming about 170 to 250 μm longer than cells in the same position of W-grown hypocotyls (Fig. 7, Col-0 panels). These results indicate that the shade-induced hypocotyl elongation of wild-type seedlings resulted from a bell-shaped non-symmetrical (skewed) elongation pattern of epidermal cells peaking around Cells 7 to 8 from the base. A skewed distribution of cell elongation in the hypocotyl has also been observed in dark-, W-, or low blue-grown hypocotyls of *A. thaliana* (Gendreau et al. 1997; Keuskamp et al. 2010), shade-exposed *B. rapa* hypocotyls (Procko et al. 2014), and end-of-day-FR-treated cowpea epicotyls (Martínez-García and García-Martínez 1992).

Independently of the primary site of action of the studied SAS regulators (e.g. cotyledons or hypocotyls), their activities converge on the elongation of hypocotyls. To establish whether the convergence affected the same or different hypocotyl cells, we next analyzed the shade-induced cell length in hypocotyls of seedlings deficient in specific SAS regulators (Supplementary Fig. S5; Fig. 7). The hyporesponsive *sav3* hypocotyls showed a similar pattern of cell elongation as wild type but strongly attenuated and slightly shifted to lower cells (elongation peak in Cells 5 to 7 that elongated $\sim 40 \mu\text{m}$ more than

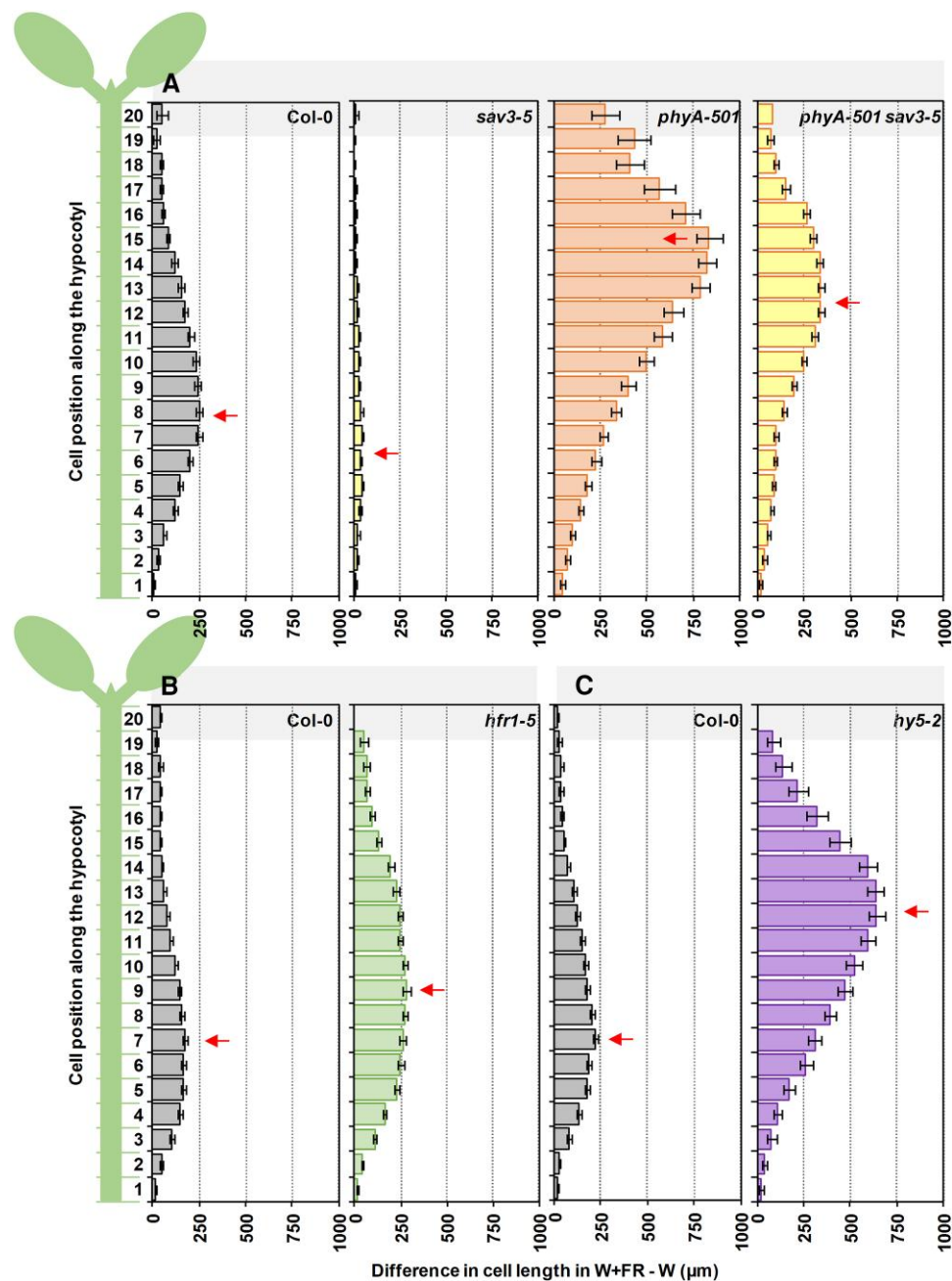


Figure 7. Distribution of the epidermal cell length from base to top induced by simulated shade in hypocotyls of wild-type or SAS mutant seedlings. Schematic representation of the 20 cells composing a cell row of the epidermis along the longitudinal axis of an *A. thaliana* hypocotyl (left). Difference in length in simulated shade (W + FR) and W for each of the 20 epidermal cells in hypocotyls of Col-0, **A)** *sav3-5*, *phyA-501*, *phyA-501 sav3-5*, **B)** *hfr1-5*, and **C)** *hy5-2*. Seedlings were grown as in Fig. 2A. Arrows point to cell with a highest difference in length. Values have been estimated after mean lengths of at least 15 cells of 2 cell rows per hypocotyl from 7 different hypocotyls per genotype and growth condition. Error bars represent se.

the same cells in W-grown hypocotyls) (Fig. 7A). In the shade-hyperresponsive *hfr1* seedlings, the peak of cell length was widened, with Cell 9 showing the maximum of elongation (~280 µm longer than Cell 9 in W-grown hypocotyls) (Fig. 7B). In the case of *hy5* and *phyA*, also hyperresponsive to shade, cell length was strongly enhanced and the elongation peak moved to the upper half of the hypocotyl (Cell 12 in *hy5* that elongated ~640 µm more than the same cell in W-grown hypocotyls; Cell 15 in *phyA* that elongated ~830 µm more than the same cell in W-grown hypocotyls) (Fig. 7, A and C).

As the peak cell number was associated with the difference in hypocotyl length in W + FR and W ($HYP_{W+FR} - HYP_W$) (Supplementary Fig. S6), we wondered if the redistribution of cell growth was a

consequence of the enhanced hypocotyl shade-induced elongation shown by these genotypes. To check this possibility, we analyzed the cell length in *phyA sav3* hypocotyls, whose shade-induced hypocotyl elongation was similar to that of *hfr1* and lower than *hy5* hypocotyls (Fig. 6). The peak of cell elongation in *phyA sav3* seedlings (Cell 13) was closer to that of *hy5* (Cell 12) and *phyA* (Cell 15). In addition, the most responsive cell in *phyA sav3* seedlings elongated more (Cell 13, ~340 µm) than in *hfr1* (Cell 9, ~280 µm). These results reinforced the conclusion that *phyA* acted by repressing the elongation of a group of cells located in the upper half of the hypocotyl (Fig. 7A). In this case, peak cell number did not associate with the $HYP_{W+FR} - HYP_W$ (Supplementary Fig. S6).

Altogether, these analyses indicate that (i) the hypocotyl cells more responsive to simulated shade are located in the lower half of the wild-type hypocotyls (centered in Cells 7 to 8), (ii) deficiency in SAS-negative regulators keeps the pattern of epidermal cell length but affects the peak cell number, and (iii) although the target cells of the various SAS-negative regulators overlap, the peak cell number due to loss of *HY5* and *PHYA* function is strongly shifted toward the upper half of the hypocotyl. These results are consistent with *phyA* and *HY5* activities repressing the cells of the upper part of the hypocotyl whereas *HFR1* more clearly repressed the elongation of cells located in the lower half of the hypocotyl, providing a spatial framework that separates the action of the participating components.

PIF457 and HY5 modulate the expression of shared shade-regulated genes

Despite the temporal differences observed between *phyA*, *HY5*, and PIFs/*HFR1*/*SAV3*, their activities overlap and eventually converge in controlling hypocotyl elongation. Hence, we aimed to further investigate possible convergence points between these 2 groups of regulators. Evidence in other photomorphogenic or temperature-regulated responses showing that *HY5* directly interacts with PIF1/PIF3 proteins (Chen et al. 2013) and *HY5* and PIF activities converge at a shared cis-regulatory element (Toledo-Ortiz et al. 2014; Gangappa and Kumar 2017; Zhang et al. 2017) led us to explore shade-induced changes of PIF457 and *HY5* in the expression of shared targets genes. We focused on 1-AMINO-CYCLOPROPANE-1-CARBOXYLATE SYNTHASE 8 (*ACS8*) and *PAR1*, identified as both potentially putative *HY5* binding targets (Lee et al. 2007) and direct PIFs targets (Khanna et al. 2007; Gallego-Bartolome et al. 2011; Yang et al. 2018). The expression of both genes was significantly promoted in *Col-0* after 1 to 8 h of W + FR treatment (compared to the beginning of the treatment) and decreased after 24 h of the shade treatment (Fig. 8). In *hy5*, *ACS8*, and *PAR1*, expression was also induced after 1 to 8 h. By contrast, in *pif457* and *hy5 pif457*, the expression of *ACS8* and *PAR1* remained virtually unaffected by the W + FR treatment (Fig. 8B). These results suggest that PIF457 activates whereas *HY5* represses *ACS8* and *PAR1* expression. Importantly, *HY5* activity depends on PIF457 transcriptional activation. These expression analyses were carried out in 7-d-old seedlings. These older seedlings elongated mildly to W + FR treatments (Supplementary Fig. S7), although the profile of response was consistent to what was observed in younger seedlings (Fig. 4H) suggesting that the same genetic components and molecular mechanisms are still functional.

To expand our understanding of the role and interaction of *HY5* and PIF457 activities, we carried out RNA sequencing (RNA-seq) of the time points 0, 1, and 8 h after shade exposure of the 4 genotypes (*Col-0*, *hy5*, *pif457*, and *hy5 pif457*) (Fig. 9A). We identified differentially expressed genes (DEGs) upregulated (fold change [FC] ≥ 1.5 , $P < 0.05$) and downregulated ($FC \leq 0.667$, $P < 0.05$) after 1 and 8 h of shade treatment compared to 0 h for each genotype analyzed (Supplementary Tables S1 to S4). After 1 h of W + FR, 386 and 791 DEGs were induced and 177 and 351 were repressed in wild-type and *hy5* seedlings, respectively. Importantly, only 1 and 3 DEGs were induced and 31 and 17 were repressed in *pif457* and *hy5 pif457* seedlings, respectively (Fig. 9, B to E). From these early shade-modulated DEGs, 294 upregulated genes were shared between *hy5* (out of 791 genes, 37.2%) and *Col-0* (out of 386 genes, 76.2%) (Fig. 9D) and 100 downregulated genes were shared between *hy5* (out of 351, 28.5%) and *Col-0* (out of 674, 14.8%) (Fig. 9E). As 748 DEGs (497 upregulated and 251 downregulated) appeared only in *hy5* but not in *Col-0*, we concluded that *HY5*

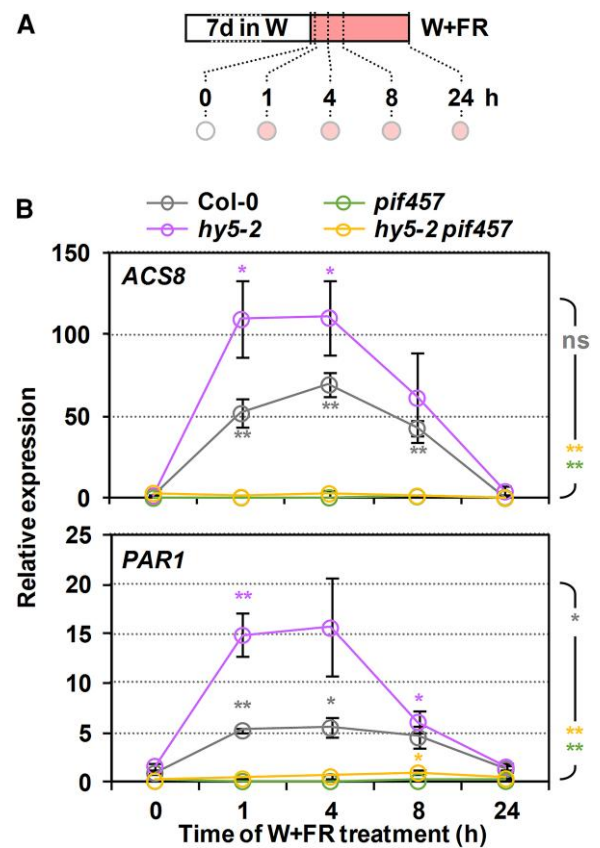


Figure 8. Effect of *hy5* and *pif457* mutations on the shade regulation of the expression of *ACS8* and *PAR1*. **A)** Cartoon of the experiment design. Seeds were grown for 7 d under W and then transferred to simulated shade (W + FR, R:FR = 0.02) for the indicated time before harvesting samples (circles). **B)** Relative expression of *ACS8* (top) and *PAR1* (bottom) in *Col-0*, *hy5-2*, *pif457*, and *hy5-2 pif457* at the indicated times of simulated shade treatment. Values are means and error bars are \pm SE of 3 independent biological replicates. Expression is presented relative to the *Col-0* genotype at 0 h. Asterisks around the symbols indicate significant differences (Student's t-test) relative to the same genotype at 0 h. Asterisk at the right indicate significant differences between the different mutants and the wild type in response to simulated shade (2-way ANOVA); ns, not significant, * $P < 0.05$, ** $P < 0.01$.

has a dual role as both activating and repressing rapid shade-modulated gene expression. The vast majority of these DEGs did not change in *pif457* and *hy5 pif457* (Fig. 9, D and E), indicating that PIF457 is basically required for all the changes in gene expression that take place after 1 h of simulated shade exposure. An important but weaker impact of PIF457 on gene expression was detected after 3 h of shade exposure (Ince et al. 2022).

After 8 h of W + FR, 826 and 542 DEGs were induced and 654 and 568 were repressed in *Col-0* and *hy5* seedlings, respectively. After this time of W + FR exposure, a substantial number of DEGs were detected in *pif457* (323 upregulated and 435 downregulated) and *hy5 pif457* (279 upregulated and 690 downregulated) seedlings (Fig. 9, B to G). Venn diagrams indicated that, from the total number of DEGs identified in all genotypes (1,347 upregulated and 1,865 downregulated), a large fraction appeared as upregulated (65.9%: 416 in *Col-0*, 144 in *hy5*, 159 in *pif457*, and 168 in *hy5 pif457*) or downregulated (78.4%: 340 in *Col-0*, 319 in *hy5*, 282 in *pif457*, and 521 in *hy5 pif457*) only in 1 genotype, whereas the rest appeared in at least 2 genotypes (Fig. 9, F and G). Based on the highest significance and the enrichment fold of overlapping genes, we concluded that the set of DEGs of *hy5 pif457* (upregulated

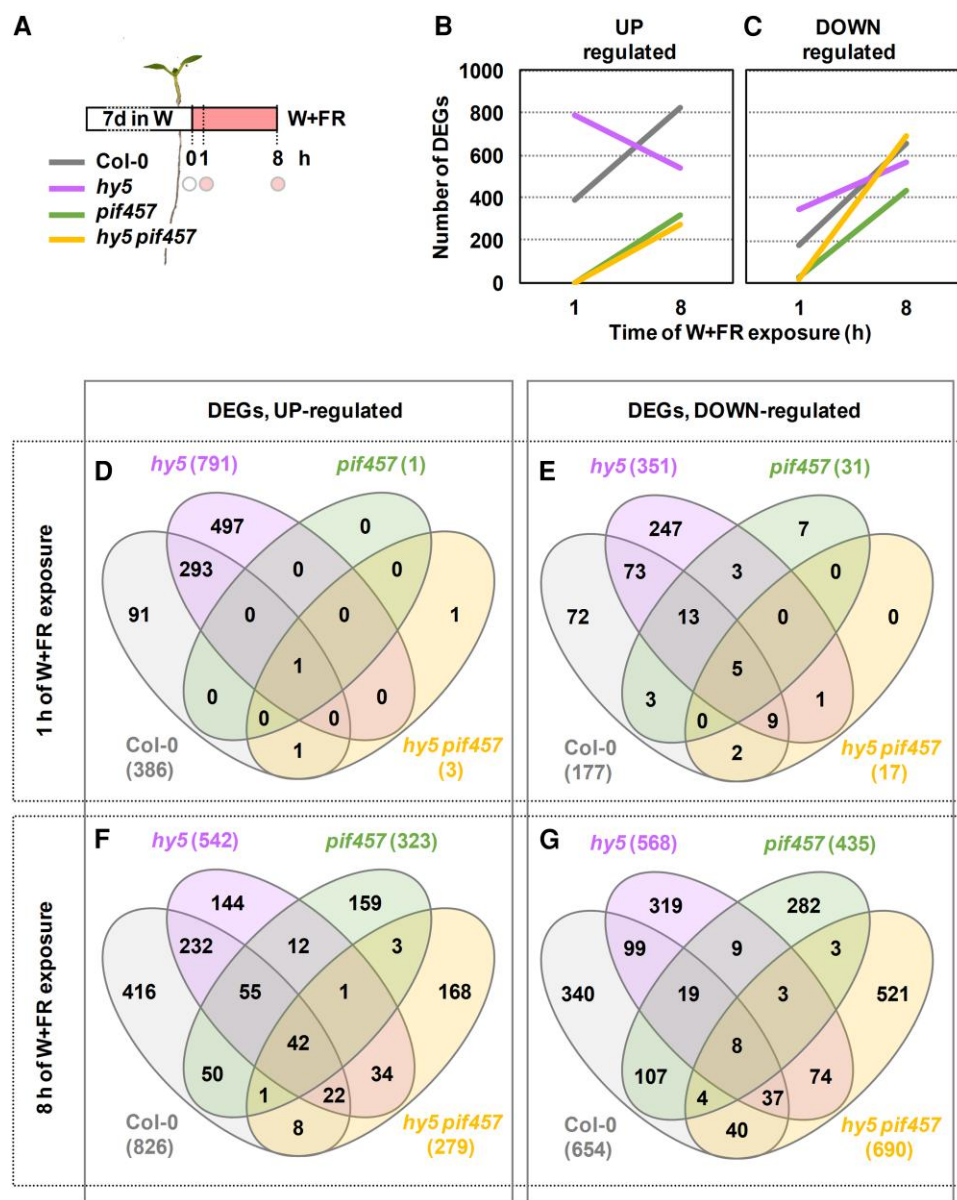


Figure 9. Effect of *hy5* and *pif457* mutations on the shade-regulated transcriptome. **A)** RNA-seq was performed with RNA extracted from Col-0, *hy5*-2, *pif457*, and *hy5*-2 *pif457* seedlings at the indicated times (circles) of simulated shade treatment. Seedlings were grown as in Fig. 8A. Three independent biological replicates were used for each genotype and treatment. Evolution of the number of upregulated **B)** and downregulated **C)** DEGs in response to 1 and 8 h of W + FR in Col-0, *hy5*-2, *pif457*, and *hy5*-2 *pif457* seedlings grown as indicated in **A)**. Venn diagrams showing the overlap of upregulated **D, F)** and downregulated **E, G)** DEGs after 1 **D, E)** and 8 h **F, G)** of W + FR treatment between Col-0, *hy5*-2, *pif457*, and *hy5*-2 *pif457* seedlings.

and downregulated) is closer to this in *hy5* than *pif457*. The number of misregulated DEGs in *hy5 pif457* is lowest when compared to *hy5* and highest when compared to *pif457* (Supplementary Fig. S8). These results indicate that, after 8 h of simulated shade, (i) the expression of a substantial amount of DEGs does not require PIF457 activity and (ii) the DEG identity is closer to *hy5* than *pif457*, in contrast to what happens at 1 h.

Regarding the functional prediction, the DEGs belonged to similar GO term categories in all genotypes (except in *pif457* and *hy5 pif457* after 1 h of W + FR, in which no GO term enrichment was found because of the massive drop in DEG number) (Supplementary Table S5). Importantly, no obvious and specific processes were differentially affected by HY5 (at 1 h) or HY5 and PIF457 at later times that could easily explain the differences in growth detected among the genotypes (Fig. 5H).

Together, we concluded that (i) PIF457 and HY5 have a strong impact in the early shade-regulated changes in gene expression, although (ii) the leading role of PIF457 at this early time of shade exposure dissipates after longer periods (8 h) of treatment.

Discussion

In the *A. thaliana* shade-induced hypocotyl elongation, the function of phyB and its effect on the PIF457-HFR1 and auxin biosynthesis via SAV3/YUCs in the cotyledons are well established (Tao et al. 2008; Li et al. 2012; Ciolfi et al. 2013; Kohlen et al. 2016; Fiorucci and Fankhauser 2017; Paulisic et al. 2021) (Fig. 1). The observed genetic interactions between *sav3/pif7/pif457* and *hfr1* (Fig. 4, A to C) and the pharmacological applications of L-kyn and NPA on *hfr1* seedlings (Fig. 5A) are consistent with this scenario. The genetic

analyses with SAS-negative and SAS-positive regulators (Figs. 2 to 4), the enhanced resistance to L-kyn and NPA shown by *phyA* and *hy5* seedlings in response to shade, and the changes in the rapid shade-induced IAA production (relative to Col-0) (Fig. 5) supported that *phyA* and *HY5* act in a different branch than *PIF457-HFR1* and *SAV3/YUCs*.

The strong shade-induced elongation of *phyA pif457* and *phyA sav3* hypocotyls (Fig. 4, D to I) indicated that these mutants, therefore, might elongate either using IAA generated from a *PIF457*- and *SAV3*-independent biosynthesis pathway or without the need of de novo synthesis of IAA. Indeed, IAA can be produced from IAA-conjugated with amino acids molecules in the hypocotyl, IAA that is able to elicit the shade-induced hypocotyl elongation independently of the *SAV3*-mediated IAA biosynthesis in cotyledons (Zheng et al. 2016). However, this increase in IAA potentially produced in the hypocotyl by this alternative pathway does not seem to be high enough for being detected when quantifying IAA in whole *phyA* or *hy5* seedlings (Fig. 5B).

HY5 is involved in the *phyA*-mediated gene repression in prolonged low R:FR (Ciolfi et al. 2013), and both *phyA* and *HY5* act very early in the seedling development (Days 2 to 5) (Fig. 6). The *phyA-HY5* early suppression seems fundamental for seedling establishment and survival soon after germination in deep shade environments (Yanovsky et al. 1995). Because deep canopy conditions are usually accompanied by reductions in the light intensity, in these early stages of the seedling development, the mechanisms of elongation are very dependent on changes of auxin sensitivity (Hersch et al. 2014) that can be modulated directly by *phyA* action on the stability of the auxin signaling repressors *Aux/IAA* (Yang et al. 2018) and by *HY5* on the promotion of the expression of negative regulators of auxin signaling (Cluis et al. 2004). The *PIF457-HFR1* module appears to be working in early and late seedling development (Fig. 6) and even in other organs and stages of development, such as petiole length and lamina size in leaves (de Wit et al. 2015), responses that appear to be more dependent on changes of auxin levels. Therefore, our results provide a temporal framework with different dependence on auxin sensitivity and levels that support the functional separation of these 2 signaling modules.

Perception of the R:FR by *phyB* in the control of the hypocotyl elongation occurs mainly in the cotyledons, where *PIF457-HFR1* promotes elongation by inducing IAA production (Tanaka et al. 2002; Keuskamp et al. 2010; Procko et al. 2014; Kohlen et al. 2016). Newly synthesized IAA is then transported to the adjacent hypocotyl where cell elongation is promoted. As before, differences were observed between the 2 signaling modules: the activity of the *PIF457-HFR1* module, that it is *SAV3*-dependent, affects the elongation of cells in the middle-lower half of the hypocotyl that is spatially distinct from that of *phyA-HY5*, that mainly represses cell elongation in the upper half (Fig. 7). It seems, therefore, that the strong repression imposed by *phyA-HY5* in the upper half of the wild-type hypocotyls takes place at the beginning of seedling development. This temporal and spatial separation of the *PIF457-HFR1* (together with *SAV3*) and *phyA-HY5* regulatory activities is consistent with an acropetal gradient of hypocotyl growth (from the base to the top) in response to simulated shade, as it was observed in both dark- and W-grown seedlings (Gendreau et al. 1997).

Additional levels of regulation refer to (i) when the different SAS components and modules act relative to the beginning of the simulated shade exposure and (ii) their level of molecular interaction. Our expression analyses indicate that *PIF457* is essential to modulate gene expression immediately after shade exposure. In clear contrast, *HY5* suppressed the number of DEGs after 1 h although its activity was strongly dependent on *PIF457* at this early time after

shade exposure (Figs. 8 and 9, D and E), which suggests a connection of the 2 mentioned branches at these initial stages after shade exposure. Previously, it has been demonstrated physical interaction between *HY5* and some *PIFs* and *HFR1* and convergence of their transcriptional activities in non-shade-related processes (Chen et al. 2013; Jang et al. 2013; Toledo-Ortiz et al. 2014; Zhang et al. 2017). Thus, *PIF457-HFR1* and *HY5* could be key players connecting the 2 regulatory modules rapidly after shade exposure. However, the crosstalk between *PIF457-HFR1* and *HY5* activities seems dynamic and changes with time. After 8 h of shade exposure, the transcriptome was clearly affected by shade even in the absence of *PIF457* (Fig. 9, B, C, F, and G), reflecting that a large percentage of the expression changes caused after shade perception by *phyB* happens bypassing *PIF457* activity. Hence, expression of these DEGs depends either on other *PIFs* (e.g. *PIF1* and *PIF3*) or on the effect exerted by unknown but non-*PIF* regulators whose transcriptional activity is also connected to the reduction in *phyB* activity caused by shade. In addition, after 8 h of shade exposure, the transcriptome divergence between the various genotypes, even between *pif457* and *hy5 pif457* (Fig. 9, F and G), points to a change in the molecular relationship of *PIFs* and *HY5* that appear in this moment to act independently from each other. What sustains this dynamic relationship is unknown, although it might involve changes in the accessibility of these regulators to the same target promoters with time triggered by shade perception (e.g. caused by the increase in the abundance of transcriptional regulators-cofactors that can affect their DNA-binding abilities), a shade-induced divergence of their spatial pattern of expression that impedes *PIFs* and *HY5* to be expressed in the same cells, and/or by epigenetic processes that alter chromatin compaction, also known to influence the accessibility and binding of transcription factors to regulatory elements in the DNA (Martínez-García and Moreno-Romero 2020).

In the SAS regulation, *PIFs* are usually presented as positive regulators by promoting the expression of genes involved in hypocotyl elongation. Our RNA-seq analyses support that they also have an important function in the repression of gene expression, as it has been previously described for some *PIFs* in shade-induced processes related with metabolic or architectural responses (hence, not related with cell elongation) (Toledo-Ortiz et al. 2010; Xie et al. 2017; Jia et al. 2020). Similarly, although *HY5* acts mainly inducing gene expression (Burko et al. 2020), it has an important role in the shade repression of genes that, after just 1 h of shade exposure, requires *PIF457* (Fig. 9, D and E).

Our findings propose a model for the regulation of shade-induced hypocotyl elongation that incorporates the temporal and spatial functional importance of the various SAS regulators analyzed in here. These components are grouped in 2 main modules or branches: (i) a well-defined pathway in which *PIF457-HFR1* participates, it is highly dependent on auxin produced via *SAV3* and *YUCs* mostly in the cotyledons, acts along all seedling development (from Days 2 to 7 from germination), and targets cells in the middle-lower region of the hypocotyl; and (ii) a less well-characterized pathway with *phyA* and *HY5* as main components, that is less dependent on *SAV3*-related auxin biosynthesis and polar transport, it has an important role in the early seedlings development (Days 2 to 5 after germination) and targets cells in the upper region of the hypocotyl. In these processes, *PIF457* transcriptional activity is fundamental at 1 h of W + FR and its importance dissipates at later times (8 h). By contrast, the importance of *HY5* regulatory role increases at longer times of shade exposure, when its expression is also reported to enhance (Ciolfi et al. 2013), likely because of the delayed accumulation of *phyA*. Importantly, the molecular interaction between these transcriptional regulators is dynamic and moves

from epistasis, soon after shade exposure, to additivity, at later hours (based on both transcriptomic and hypocotyl elongation experiments). Because of the reported interaction of HY5 with some PIFs and HFR1, it might act connecting both branches that, therefore, are crosstalking along the seedling development.

Materials and methods

Plant material and growth conditions

All the *A. thaliana* plant material used was in the Col-0 background. Mutants used in this study were described before: *phyA-501* (Martínez-García et al. 2014), *hy5-2* (Ortiz-Alcaide et al. 2019), *hfr1-5* (Roig-Villanova et al. 2007), *pif7-1* (Li et al. 2012), and *sav3-5*, also known as *wei8-4/tir2-3* (Stepanova et al. 2008). The multiple mutants *pif457* (*pif4-101 pif5-3 pif7-1*) (de Wit et al. 2015), *phyA-211 hfr1-101* (Duek et al. 2004), and *phyA-211 phyB-9* (Strasser et al. 2010) used in this study were described elsewhere. To produce seeds of the various *A. thaliana* genotypes, plants were grown in the greenhouse under long day photoperiod (16-h light, 8-h dark).

Fluence rates were measured with a Spectrosense2 meter associated with a 4-channel sensor (Skye Instruments Ltd., www.skyeinstruments.com), which measures PAR (400 to 700 nm) and 10-nm windows in the blue (464 to 473 nm), R (664 to 674 nm), and FR (725 to 735 nm) regions. Light spectra were generated using a Flame Model Spectrometer with Sony Detector (FLAME-S; Ocean Optics).

Pharmacological treatments

When indicated, the medium was supplemented with different concentrations of L-kyn (Sigma-Aldrich) or NPA (Duchefa). L-kyn was dissolved at 50 mM in DMSO. NPA was dissolved at 5 mM in DMSO. Stock solutions were kept at -20°C until use.

Genetic crosses and genotyping

Mutants were crossed to generate the following multiple mutants: *phyA hy5* (*phyA-501 hy5-2*), *phyA pif7* (*phyA-501 pif7-1*), *phyA hfr1* (*phyA-501 hfr1-5*), *phyA sav3* (*phyA-501 sav3-5*), *hy5 pif7* (*hy5-2 pif7-1*), *hy5 hfr1* (*hy5-2 hfr1-5*), *hy5 sav3* (*hy5-2 sav3-5*), *hfr1 pif7* (*hfr1-5 pif7-1*), *hfr1 pif457* (*hfr1-5 pif457*), *hy5 pif457* (*hy5-2 pif457*), and *phyA pif457* (*phyA-501 pif457*). After crosses, seedlings in the segregating F2 generation were preselected searching by the predicted phenotypes, if any. In any case, the genetic identity of the plants was established by genotyping the preselected plants by PCR using specific primers (Supplementary Table S6).

Measurements of hypocotyl length

For hypocotyl growth assays, seeds were sterilized and sown in solid agar plates without sucrose (GM–; 0.215% [*w/v*] MS salts plus vitamins, 0.025% [*w/v*] MES pH 5.80) (Roig-Villanova et al. 2019). After 3 to 6 d of stratification, plates were incubated in growth chambers at 22°C under continuous W provided by 4 cool-white vertical fluorescence tubes (F36W/840, Sylvania) for 2 d (PAR of 20 to $25\ \mu\text{mol}\cdot\text{m}^{-2}\cdot\text{s}^{-1}$, R:FR > 2.5). After that time, plates were either maintained in W or transferred to simulated shade (W + FR) for 5 d. Simulated shade was generated by enriching W with supplementary FR (peak at 725 nm) provided by 4 horizontal LED lamps (Philips GreenPower LED module FR) (PAR of 20 to $25\ \mu\text{mol}\cdot\text{m}^{-2}\cdot\text{s}^{-1}$, R:FR of about 0.02). Details of the resulting light spectra are shown as Supplementary Fig. S9 (Molina-Contreras et al. 2019). At Day 7, seedlings were flattened down on the petri dishes and pictures of them were taken. Each biological replicate corresponded to ~25 seedlings per treatment and genotype. Experiments were done with at least 3

biological replicates. Hypocotyl measurements were carried out by using the National Institutes of Health (NHS) ImageJ software (Bethesda, MD, USA; <http://rsb.info.nih.gov>). Hypocotyl measurements from the different biological replicates were averaged.

Hypocotyl measurements for the temporal analyses

Seedlings were grown for up to 7 d either in W or W + FR, as described in the previous section. In these experiments (Fig. 6; Supplementary Fig. S3), hypocotyl length measurements were made daily from pictures taken from plants of different ages, from Day 2 until Day 7 after germination (6 time points). By subtracting the hypocotyl length of 2 consecutive days, the growth rate ($\text{mm}\cdot\text{day}^{-1}$) from Days 2 to 6 was calculated for each genotype and light treatment (W and W + FR). Each biological replicate corresponded to ~25 seedlings per treatment, genotype, and time point. Experiments were done with 3 biological replicates. Hypocotyl measurements from the different biological replicates were averaged. These averaged data were used to calculate the growth rate.

Hormone analyses

About 50 seedlings per biological replica of the different genotypes and treatments (that ranged from 80 to 120 mg) were immediately frozen in liquid nitrogen. Hormone extraction and analysis were performed as described (Simura et al. 2018) with a few modifications. Briefly, around 100 mg of fresh material was extracted in 1 mL of 50% (*v/v*) acetonitrile prepared with ultrapure water, adding 2.5 ng of [$^2\text{H}_5$]IAA as internal standard in a ball mill (MillMix 20, Domel) for 10 min at 17 rps, followed by 5 min of sonication. After sonication, the samples were centrifuged at $4,000 \times g$ at 4°C for 10 min. Finally, supernatants were filtered through SPE columns (OASIS HLB 30 mg 1 cc, Waters), recovering the eluent. Finally, 0.5 mL of 30% (*v/v*) acetonitrile prepared in ultrapure water was added to the SPE columns and the eluent was recovered joint to the previous ones.

Chromatographic separations were performed on a reverse-phase C18 column ($50 \times 2.1\ \text{mm}$, $1.6\text{-}\mu\text{m}$ particle size, Luna-Omega, Phenomenex) using a acetonitrile:water (both supplemented with 0.1% [*v/v*] formic acid) gradient at a flow rate of $300\ \mu\text{L}/\text{min}$. IAA was detected with a triple quadrupole mass spectrometer connected online to the output of the column through an orthogonal Z-spray electrospray ion source (Xevo TQ-S). Finally, IAA content was quantified by interpolation in a standard curve prepared with commercial IAA (Sigma) using the MassLynx v4.2 software.

Cell length measurements along the hypocotyl axis for spatial analysis

For the cell length measurements, about 100 seedlings were grown either in W or W + FR, as previously described. On Day 7, hypocotyls were measured and the mean value for each group (genotype and treatment) was calculated. About 15 individuals with a hypocotyl length of the estimated averaged value $\pm 5\%$ were selected. Cotyledons and roots were removed from these seedlings and the remaining hypocotyls were fixed and stained with Calcofluor White (Sigma-Aldrich) to visualize cell walls. Briefly, hypocotyls were submerged in a $1 \times$ PBS solution ($137\ \text{mM}$ NaCl [$8.06\ \text{g/L}$], $2.7\ \text{mM}$ KCl [$0.22\ \text{g/L}$], $10\ \text{mM}$ Na_2HPO_4 [$1.15\ \text{g/L}$], $18\ \text{mM}$ KH_2HPO_4 [$0.20\ \text{g/L}$]) with 4% (*w/v*) paraformaldehyde for 60 min at room temperature. Then, hypocotyls were washed twice for 1 min in $1 \times$ PBS and cleared after transferring them to ClearSee solution (10% [*w/v*] xylitol [Sigma], 15% [*w/v*] sodium deoxycholate [Sigma], 25% [*w/v*] urea [Sigma]). The clearing was carried out for at least

1 wk at room temperature. Before taking images, hypocotyls were stained with $100 \mu\text{g}\cdot\text{mL}^{-1}$ Calcofluor in ClearSee solution for 120 min and washed twice with ClearSee solution for 2 d (Kurihara et al. 2015).

Images of fixed and stained plant material were taken by using confocal microscopy (Zeiss LSM 780). Calcofluor White stained samples were imaged with 405-nm excitation Argon laser and detected at 425 to 475 nm (Kamiya et al. 2015). In most of the images, gain and laser intensity were adjusted to remove background noise. Cell growth measurements were carried out using the NHS ImageJ software on the obtained pictures. At least 15 cells of 2 cell files per hypocotyl from 7 seedlings were measured for each genotype and growth condition. Values were averaged for each of the about 20 cells that constitute a cell file (from bottom to top) along the hypocotyl longitudinal axis.

RNA extraction and gene expression analyses

Seven-day-old seedlings grown in W or W+FR were harvested (about 35 mg per sample) and frozen in liquid nitrogen. RNA was extracted using commercial kits (Maxwell RSC Plant RNA kits; www.promega.com) and quantified using NanoDropTM 8000 spectrophotometer (Thermo Fisher Scientific). Two micrograms of total RNA were retrotranscribed to cDNA in a final volume of 20 μL by using the Transcriptor First Strand cDNA Synthesis Kit (Roche, www.roche.com) or the NZY First-Strand cDNA Synthesis Kit, separate oligos (NZYtech) following the manufacturer's instructions. Subsequently, cDNA was diluted 10-fold and stored at -20°C for further analysis.

Relative mRNA abundance was determined via reverse transcription quantitative PCR (RT-qPCR) in a final volume of 10 μL made up of 0.3 μM of both forward and reverse primers, 5 μL of the LightCycler 480 SYBR Green I Master Mix (Roche), and 2 μL of 10-fold diluted cDNA (Molina-Contreras et al. 2019). The RT-qPCR was carried out in LightCycler 480 Real-Time PCR system (Roche). The analysis was performed with 3 independent biological replicates (~30 seedlings per biological replicate) for each condition and 3 technical replicates for each biological replicate. *ELONGATION FACTOR 1 α* (*EF1 α*) was used as endogenous reference genes to normalize the expression of the genes of interest. Primers used for the RT-qPCR analyses are provided in [Supplementary Table S7](#).

Statistical analyses

These analyses were carried out using the Real Statistics Resource Pack, an Excel add-in that extends Excel's standard statistics capabilities. For the statistical analyses, we compared 3 values corresponding to 3 replicates in the case of relative expression and hypocotyl length.

RNA-seq: processing, analyses, and data availability

Total RNA for sequencing was obtained as in the expression analyses by RT-qPCR. The total RNA samples were quantified using the Qubit RNA BR Assay Kit (Thermo Fisher Scientific), and the RNA integrity was assessed with the Agilent RNA 6000 Pico Bioanalyzer 2100 Assay (Agilent).

The RNA-seq libraries were prepared using the KAPA Stranded mRNA-Seq Illumina Platforms Kit (Roche), following the manufacturer's recommendations, starting with 500 ng of total RNA. The size and quality of the libraries were evaluated using a High Sensitivity DNA Bioanalyzer assay (Agilent). The libraries were sequenced on the HiSeq 4000 (Illumina) with a read length of 2×51 bp using the HiSeq 4000 SBS Kit (Illumina), following the

manufacturer's protocol for dual indexing. Image analysis, base calling, and quality scoring of the run were performed using the manufacturer's software Real Time Analysis (RTA 2.7.7). RNA-seq data have been deposited in NCBI's Gene Expression Omnibus (GEO) and are accessible through GEO Series accession number [GSE268032](https://www.ncbi.nlm.nih.gov/geo/query/acc.cgi?acc=GSE268032).

RNA-seq reads were mapped against *A. thaliana* reference genome (TAIR10) from Ensembl Plants, using STAR aligner version 2.5.3a (Dobin et al. 2013) and ENCODE parameters. Annotated genes were quantified with RSEM v1.3.0 (Li and Dewey 2011), using Ensembl annotation release 47. Differential expression analysis was performed with limma v3.4.2 R package. Counts were normalized with TMM (Robinson and Oshlack 2010) and transformed with the "voom" function. The linear model was fitted with the voom-transformed counts and contrasts were extracted. Genes were considered differentially expressed (DEG) with an adjusted $P < 0.05$. From these, we selected those whose $0.667 \geq FC \geq 1.5$.

GO enrichment

The list of DEGs ([Supplementary Tables S1 to S4](#)) was used to identify the enrichment in GO terms using the agriGO online analyses tool.

Accession numbers

Sequence data from this article can be found in the GenBank/EMBL data libraries under accession numbers ACS8 (At4g37770), *EF1 α* (At5g60390), *HFR1* (At1g02340), *HY5* (At5g11260), *PAR1* (At2g42870), *PHYA* (At1g09570), *PHYB* (At2g18790), *PIF4* (At2G43010), *PIF5* (At3g59060), *PIF7* (At5g61270), and *SAV3* (At1g70560).

Acknowledgments

We are grateful to Christian Fankhauser (University of Lausanne, Switzerland) for providing *pif457* and *phyA-211 hfr1-101* seeds, to Pablo Cerdán (Fundación Instituto Leloir, Argentina) for providing *phyA-211 phyB-9* seeds, to Javier Brumós (IBMCP) for comments on the manuscript, and to Javier Forment (IBMCP) for helping in GEO data submission.

Author contributions

J.F.M.-G. designed the research; P.P.-A., J.M.-R., J.P.-R., S.P., E.K., V.V.-P., A.G.-C., and A.R.-V. performed the research and analyzed their respective data; A.E.-C. and B.M.-M. performed and analyzed RNA-seq data; J.F.M.-G., P.P.-A., and J.M.-R. wrote the paper with revisions, contributions, and/or comments from all other authors.

Supplementary data

The following materials are available in the online version of this article.

Supplementary Figure S1. Genetic interaction of SAS negative regulators in the shade-induced hypocotyl elongation.

Supplementary Figure S2. Genetic interaction of pairs of SAS-negative and -positive regulators in the shade-induced hypocotyl elongation.

Supplementary Figure S3. Effect of *phyA*, *phyB*, *HFR1*, and *HY5* mutations on the hypocotyl growth rate under W and simulated shade.

Supplementary Figure S4. Representative confocal images of Col-0 hypocotyls grown under W or simulated shade to measure epidermal cell length.

Supplementary Figure S5. Distribution of the epidermal cell length from base to top induced by simulated shade in hypocotyls of wild-type or SAS mutant seedlings.

Supplementary Figure S6. Correlation between peak of cell number and difference in length in simulated shade and W-grown hypocotyls.

Supplementary Figure S7. Effect of *hy5* and *pif457* mutations on the shade-induced hypocotyl elongation of older seedlings.

Supplementary Figure S8. Overlap of upregulated and down-regulated gene groups between Col-0, *hy5*, *pif457*, and *hy5 pif457* after 8 h of shade treatment.

Supplementary Figure S9. Light spectra of the treatments given in this study.

Supplementary Table S1. Bioset of upregulated DEGs in Col-0 seedlings in response to 1 to 8 h of W + FR.

Supplementary Table S2. Bioset of upregulated DEGs in *hy5* seedlings in response to 1 to 8 h of W + FR.

Supplementary Table S3. Bioset of upregulated DEGs in *pif457* seedlings in response to 1 to 8 h of W + FR.

Supplementary Table S4. Bioset of upregulated DEGs in *hy5 pif457* seedlings in response to 1 to 8 h of W + FR.

Supplementary Table S5. Functional enrichment groups based on GO term analyses.

Supplementary Table S6. Primers used for genotyping the different lines.

Supplementary Table S7. Primers used for gene expression analyses.

Funding

P.P.-A. was funded by a short-term EMBO fellowship that covered his stay at the ETH, Zurich. J.M.-R. has received funding from the European Union's Horizon 2020 research and innovation program under the Marie Skłodowska-Curie (H2020-MSCA-IF-2017) grant agreement 797473. J.P.-R. is supported by a predoctoral fellowship from Agencia Estatal de Investigación (PRE2021-099195). M.U.-B. is supported by a predoctoral fellowship from the Spanish Ministerio de Universidades (FPU20/05486). Our research is supported by grants BIO2017-85316-R from MCIN/AEI/10.13039/501100011033, "ERDF A way of making Europe", PID2020-115782GB-I00 from MCIN/AEI/10.13039/501100011033, PROMETEU/2021/065 from Generalitat Valenciana, and the EC-H2020-PRIMA UToPIQ project (PCI2021-121941) funded by Agencia Estatal de Investigación. We also acknowledge the support of the CERCA Programme/Generalitat de Catalunya.

Conflict of interest statement. None declared.

References

- Bou-Torrent J, Toledo-Ortiz G, Ortiz-Alcaide M, Cifuentes-Esquivel N, Halliday KJ, Martinez-Garcia JF, Rodriguez-Concepcion M. Regulation of carotenoid biosynthesis by shade relies on specific subsets of antagonistic transcription factors and cofactors. *Plant Physiol.* 2015;169(3):1584–1594. <https://doi.org/10.1104/pp.15.00552>
- Brumos J, Alonso JM, Stepanova AN. Genetic aspects of auxin biosynthesis and its regulation. *Physiol Plant.* 2014;151(1):3–12. <https://doi.org/10.1111/pp.12098>
- Burko Y, Seluzicki A, Zander M, Pedmale UV, Ecker JR, Chory J. Chimeric activators and repressors define HY5 activity and reveal a light-regulated feedback mechanism. *Plant Cell.* 2020;32(4):967–983. <https://doi.org/10.1105/tpc.19.00772>
- Buti S, Pantazopoulou CK, van Gelderen K, Hoogers V, Reinen E, Pierik R. A gas-and-brake mechanism of bHLH proteins modulates shade avoidance. *Plant Physiol.* 2020;184(4):2137–2153. <https://doi.org/10.1104/pp.20.00677>
- Casal JJ. Shade avoidance. *Arabidopsis Book.* 2012;10:e0157. <https://doi.org/10.1199/tab.0157>
- Chen F, Li B, Li G, Charron JB, Dai M, Shi X, Deng XW. Arabidopsis phytochrome a directly targets numerous promoters for individualized modulation of genes in a wide range of pathways. *Plant Cell.* 2014;26(5):1949–1966. <https://doi.org/10.1105/tpc.114.123950>
- Chen D, Xu G, Tang W, Jing Y, Ji Q, Fei Z, Lin R. Antagonistic basic helix-loop-helix/bZIP transcription factors form transcriptional modules that integrate light and reactive oxygen species signaling in Arabidopsis. *Plant Cell.* 2013;25(5):1657–1673. <https://doi.org/10.1105/tpc.112.104869>
- Cifuentes-Esquivel N, Bou-Torrent J, Galstyan A, Gallemi M, Sessa G, Salla Martret M, Roig-Villanova I, Ruberti I, Martinez-Garcia JF. The bHLH proteins BEE and BIM positively modulate the shade avoidance syndrome in Arabidopsis seedlings. *Plant J.* 2013;75(6):989–1002. <https://doi.org/10.1111/tpj.12264>
- Ciolfi A, Sessa G, Sassi M, Possenti M, Salvucci S, Carabelli M, Morelli G, Ruberti I. Dynamics of the shade-avoidance response in Arabidopsis. *Plant Physiol.* 2013;163(1):331–353. <https://doi.org/10.1104/pp.113.221549>
- Cluis CP, Mouchel CF, Hardtke CS. The Arabidopsis transcription factor HY5 integrates light and hormone signaling pathways. *Plant J.* 2004;38(2):332–347. <https://doi.org/10.1111/j.1365-313X.2004.02052.x>
- Devlin PF, Yanovsky MJ, Kay SA. A genomic analysis of the shade avoidance response in Arabidopsis. *Plant Physiol.* 2003;133(4):1617–1629. <https://doi.org/10.1104/pp.103.034397>
- de Wit M, Keuskamp DH, Bongers FJ, Hornitschek P, Gommers CMM, Reinen E, Martinez-Ceron C, Fankhauser C, Pierik R. Integration of phytochrome and cryptochrome signals determines plant growth during competition for light. *Curr Biol.* 2016;26(24):3320–3326. <https://doi.org/10.1016/j.cub.2016.10.031>
- de Wit M, Ljung K, Fankhauser C. Contrasting growth responses in lamina and petiole during neighbor detection depend on differential auxin responsiveness rather than different auxin levels. *New Phytol.* 2015;208(1):198–209. <https://doi.org/10.1111/nph.13449>
- Dobin A, Davis CA, Schlesinger F, Drenkow J, Zaleski C, Jha S, Batut P, Chaisson M, Gingeras TR. STAR: ultrafast universal RNA-seq aligner. *Bioinformatics.* 2013;29(1):15–21. <https://doi.org/10.1093/bioinformatics/bts635>
- Duek PD, Elmer MV, van Oosten VR, Fankhauser C. The degradation of HFR1, a putative bHLH class transcription factor involved in light signaling, is regulated by phosphorylation and requires COP1. *Curr Biol.* 2004;14(24):2296–2301. <https://doi.org/10.1016/j.cub.2004.12.026>
- Fairchild CD, Schumaker MA, Quail PH. HFR1 encodes an atypical bHLH protein that acts in phytochrome A signal transduction. *Genes Dev.* 2000;14(8):2377–2391. www.genesdev.org/cgi/doi/10.1101/gad.82800
- Fiorucci AS, Fankhauser C. Plant strategies for enhancing access to sunlight. *Curr Biol.* 2017;27(17):R931–R940. <https://doi.org/10.1016/j.cub.2017.05.085>
- Gallego-Bartolome J, Arana MV, Vandenbussche F, Žádníková P, Minguet EG, Guardiola V, Van Der Straeten D, Benkova E, Alabádi D, Blázquez MA. Hierarchy of hormone action controlling apical hook development in Arabidopsis. *Plant J.* 2011;67(4):622–634. <https://doi.org/10.1111/j.1365-313X.2011.04621.x>

- Gallelli M, Galstyan A, Paulisic S, Then C, Ferrandez-Ayela A, Lorenzo-Orts L, Roig-Villanova I, Wang X, Micol JL, Ponce MR, et al. DRACULA2 is a dynamic nucleoporin with a role in regulating the shade avoidance syndrome in *Arabidopsis*. *Development*. 2016;143(9):1623–1631. <https://doi.org/10.1242/dev.130211>
- Gallelli M, Molina-Contreras MJ, Paulisic S, Salla-Martret M, Sorin C, Godoy M, Franco-Zorrilla JM, Solano R, Martinez-Garcia JF. A non-DNA-binding activity for the ATHB4 transcription factor in the control of vegetation proximity. *New Phytol*. 2017;216(3):798–813. <https://doi.org/10.1111/nph.14727>
- Galstyan A, Cifuentes-Esquivel N, Bou-Torrent J, Martinez-Garcia JF. The shade avoidance syndrome in *Arabidopsis*: a fundamental role for atypical basic helix-loop-helix proteins as transcriptional cofactors. *Plant J*. 2011;66(2):258–267. <https://doi.org/10.1111/j.1365-313X.2011.04485.x>
- Gangappa SN, Crocco CD, Johansson H, Datta S, Hettiarachchi C, Holm M, Botto JF. The *Arabidopsis* B-BOX protein BBX25 interacts with HY5, negatively regulating BBX22 expression to suppress seedling photomorphogenesis. *Plant Cell*. 2013;25(4):1243–1257. <https://doi.org/10.1105/tpc.113.109751>
- Gangappa SN, Kumar SV. DET1 and HY5 control PIF4-mediated thermosensory elongation growth through distinct mechanisms. *Cell Rep*. 2017;18(2):344–351. <https://doi.org/10.1016/j.celrep.2016.12.046>
- Gendreau E, Traas J, Desnos T, Grandjean O, Caboche M, Hofte H. Cellular basis of hypocotyl growth in *Arabidopsis thaliana*. *Plant Physiol*. 1997;114(1):295–305. <https://doi.org/10.1104/pp.114.1.295>
- Gommers CM, Keuskamp DH, Buti S, van Veen H, Koevoets IT, Reinen E, Voesenek LA, Pierik R. Molecular profiles of contrasting shade response strategies in wild plants: differential control of immunity and shoot elongation. *Plant Cell*. 2017;29(2):331–344. <https://doi.org/10.1105/tpc.16.00790>
- He W, Brumos J, Li H, Ji Y, Ke M, Gong X, Zeng Q, Li W, Zhang X, An F, et al. A small-molecule screen identifies L-kynurenine as a competitive inhibitor of TAA1/TAR activity in ethylene-directed auxin biosynthesis and root growth in *Arabidopsis*. *Plant Cell*. 2011;23(11):3944–3960. <https://doi.org/10.1105/tpc.111.089029>
- Hersch M, Lorrain S, de Wit M, Trevisan M, Ljung K, Bergmann S, Fankhauser C. Light intensity modulates the regulatory network of the shade avoidance response in *Arabidopsis*. *Proc Natl Acad Sci U S A*. 2014;111(17):6515–6520. <https://doi.org/10.1073/pnas.1320355111>
- Hornitschek P, Kohnen MV, Lorrain S, Rougemont J, Ljung K, López-Vidriero I, Franco-Zorrilla JM, Solano R, Trevisan M, Pradervand S, et al. Phytochrome interacting factors 4 and 5 control seedling growth in changing light conditions by directly controlling auxin signaling. *Plant J*. 2012;71(5):699–711. <https://doi.org/10.1111/j.1365-313X.2012.05033.x>
- Hornitschek P, Lorrain S, Zoete V, Michielin O, Fankhauser C. Inhibition of the shade avoidance response by formation of non-DNA binding bHLH heterodimers. *EMBO J*. 2009;28(24):3893–3902. <https://doi.org/10.1038/emboj.2009.306>
- Huang X, Zhang Q, Jiang Y, Yang C, Wang Q, Li L. Shade-induced nuclear localization of PIF7 is regulated by phosphorylation and 14-3-3 proteins in *Arabidopsis*. *Elife*. 2018;7:e31636. <https://doi.org/10.7554/eLife.31636>
- Ince YÇ, Krahmer J, Fiorucci AS, Trevisan M, Galvão VC, Wigger L, Pradervand S, Fouillen L, Van Delft P, Genva M, et al. A combination of plasma membrane sterol biosynthesis and autophagy is required for shade-induced hypocotyl elongation. *Nat Commun*. 2022;13(1):5659. <https://doi.org/10.1038/s41467-022-33384-9>
- Jang IC, Henriques R, Chua NH. Three transcription factors, HFR1, LAF1 and HY5, regulate largely independent signaling pathways downstream of phytochrome A. *Plant Cell Physiol*. 2013;54(6):907–916. <https://doi.org/10.1093/pcp/pct042>
- Jia Y, Kong X, Hu K, Cao M, Liu J, Ma C, Guo S, Yuan X, Zhao S, Robert HS et al. PIFs coordinate shade avoidance by inhibiting auxin repressor ARF18 and metabolic regulator QQS. *New Phytol*. 2020;228(2):609–621. <https://doi.org/10.1111/nph.16732>
- Kamiya T, Borghi M, Wang P, Danku JMC, Kalmbach L, Hosmani PS, Naseer S, Fujiwara T, Geldner N, Salt DE. The MYB36 transcription factor orchestrates Casparian strip formation. *Proc Natl Acad Sci U S A*. 2015;112(33):10533–10538. <https://doi.org/10.1073/pnas.1507691112>
- Keuskamp DH, Pollmann S, Voesenek LA, Peeters AJ, Pierik R. Auxin transport through PIN-FORMED 3 (PIN3) controls shade avoidance and fitness during competition. *Proc Natl Acad Sci U S A*. 2010;107(52):22740–22744. <https://doi.org/10.1073/pnas.1013457108>
- Khanna R, Shen Y, Marion CM, Tsuchisaka A, Theologis A, Schäfer E, Quail PH. The basic helix-loop-helix transcription factor PIF5 acts on ethylene biosynthesis and phytochrome signaling by distinct mechanisms. *Plant Cell*. 2007;19(12):3915–3929. <https://doi.org/10.1105/tpc.107.051508>
- Kim YM, Woo JC, Song PS, Soh MS. HFR1, a phytochrome A-signalling component, acts in a separate pathway from HY5, downstream of COP1 in *Arabidopsis thaliana*. *Plant J*. 2002;30(6):711–719. <https://doi.org/10.1046/j.1365-313X.2002.01326.x>
- Kohnen MV, Schmid-Siegert E, Trevisan M, Petrolati LA, Senechal F, Muller-Moule P, Maloof J, Xenarios I, Fankhauser C. Neighbor detection induces organ-specific transcriptomes. Revealing patterns underlying hypocotyl-specific growth. *Plant Cell*. 2016;28(12):2889–2904. <https://doi.org/10.1105/tpc.16.00463>
- Kurihara D, Mizuta Y, Sato Y, Higashiyama T. ClearSee: a rapid optical clearing reagent for whole-plant fluorescence imaging. *Development*. 2015;142(23):4168–4179. <https://doi.org/10.1242/dev.127613>
- Lee J, He K, Stolc V, Lee H, Figueroa P, Gao Y, Tongprasit W, Zhao H, Lee I, Deng XW. Analysis of transcription factor HY5 genomic binding sites revealed its hierarchical role in light regulation of development. *Plant Cell*. 2007;19(3):731–749. <https://doi.org/10.1105/tpc.106.047688>
- Li B, Dewey CN. RSEM: accurate transcript quantification from RNA-Seq data with or without a reference genome. *BMC Bioinformatics*. 2011;12(1):323. <https://doi.org/10.1186/1471-2105-12-323>
- Li L, Ljung K, Breton G, Schmitz RJ, Pruneda-Paz J, Cowing-Zitron C, Cole BJ, Ivans LJ, Pedmale UV, Jung HS, et al. Linking photoreceptor excitation to changes in plant architecture. *Genes Dev*. 2012;26(8):785–790. <https://doi.org/10.1101/gad.187849.112>
- Martinez-Garcia JF, Moreno-Romero J. Shedding light on the chromatin changes that modulate shade responses. *Physiol Plant*. 2020;169(3):407–417. <https://doi.org/10.1111/ppl.13101>
- Martinez-Garcia JF, Rodriguez-Concepcion M. Molecular mechanisms of shade tolerance in plants. *New Phytol*. 2023;239(4):1190–1202. <https://doi.org/10.1111/nph.19047>
- Martínez-García JF, Gallelli M, Molina-Contreras MJ, Llorente B, Bevilacqua MR, Quail PH. The shade avoidance syndrome in *Arabidopsis*: the antagonistic role of phytochrome A and B differentiates vegetation proximity and canopy shade. *PLoS One*. 2014;9(10):e109275. <https://doi.org/10.1371/journal.pone.0109275>
- Martínez-García JF, García-Martínez JL. Interaction of gibberellins and phytochrome in the control of cowpea epicotyl elongation. *Physiol Plant*. 1992;86(2):236–244. <https://doi.org/10.1034/j.1399-3054.1992.860208.x>
- Molina-Contreras MJ, Paulišić S, Then C, Moreno-Romero J, Pastor-Andreu P, Morelli L, Roig-Villanova I, Jenkins H, Hallab A, Gan X, et al. Photoreceptor activity contributes to contrasting

- responses to shade in *Cardamine* and *Arabidopsis* seedlings. *Plant Cell*. 2019;31(11):2649–2663. <https://doi.org/10.1105/tpc.19.00275>
- Morelli L, Paulišić S, Qin W, Iglesias-Sanchez A, Roig-Villanova I, Florez-Sarasa I, Rodriguez-Concepcion M, Martinez-Garcia JF. Light signals generated by vegetation shade facilitate acclimation to low light in shade-avoider plants. *Plant Physiol*. 2021;186(4):2137–2151. <https://doi.org/10.1093/plphys/kiab206>
- Ortiz-Alcaide M, Llamas E, Gomez-Cadenas A, Nagatani A, Martinez-Garcia JF, Rodriguez-Concepcion M. Chloroplasts modulate elongation responses to canopy shade by retrograde pathways involving HY5 and abscisic acid. *Plant Cell*. 2019;31(2):384–398. <https://doi.org/10.1105/tpc.18.00617>
- Pacín M, Legris M, Casal JJ. COP1 re-accumulates in the nucleus under shade. *Plant J*. 2013;75(4):631–641. <https://doi.org/10.1111/tbj.12226>
- Pacín M, Semmloni M, Legris M, Finlayson SA, Casal JJ. Convergence of CONSTITUTIVE PHOTOMORPHOGENESIS 1 and PHYTOCHROME INTERACTING FACTOR signalling during shade avoidance. *New Phytol*. 2016;211(3):967–979. <https://doi.org/10.1111/nph.13965>
- Paulisic S, Qin W, Arora Veraszto H, Then C, Alary B, Nogue F, Tsiantis M, Hothorn M, Martinez-Garcia JF. Adjustment of the PIF7-HFR1 transcriptional module activity controls plant shade adaptation. *EMBO J*. 2021;40(1):e104273. <https://doi.org/10.15252/emboj.2019104273>
- Pierik R, de Wit M. Shade avoidance: phytochrome signalling and other aboveground neighbour detection cues. *J Exp Bot*. 2014;65(11):2815–2824. <https://doi.org/10.1093/jxb/ert389>
- Procko C, Burko Y, Jaillais Y, Ljung K, Long JA, Chory J. The epidermis coordinates auxin-induced stem growth in response to shade. *Genes Dev*. 2016;30(13):1529–1541. <https://doi.org/10.1101/gad.283234.116>
- Procko C, Crenshaw CM, Ljung K, Noel JP, Chory J. Cotyledon-generated auxin is required for shade-induced hypocotyl growth in *Brassica rapa*. *Plant Physiol*. 2014;165(3):1285–1301. <https://doi.org/10.1104/pp.114.241844>
- Robinson MD, Oshlack A. A scaling normalization method for differential expression analysis of RNA-seq data. *Genome Biol*. 2010;11(3):R25. <https://doi.org/10.1186/gb-2010-11-3-r25>
- Roig-Villanova I, Bou-Torrent J, Galstyan A, Carretero-Paulet L, Portolés S, Rodríguez-Concepción M, Martínez-García JF. Interaction of shade avoidance and auxin responses: a role for two novel atypical bHLH proteins. *EMBO J*. 2007;26(22):4756–4767. <https://doi.org/10.1038/sj.emboj.7601890>
- Roig-Villanova I, Bou J, Sorin C, Devlin PF, Martínez-García JF. Identification of primary target genes of phytochrome signaling. Early transcriptional control during shade avoidance responses in *Arabidopsis*. *Plant Physiol*. 2006;141(1):85–96. <https://doi.org/10.1104/pp.105.076331>
- Roig-Villanova I, Martínez-García JF. Molecular regulation of plant responses to shade. In: Lüttge U, Cánovas FM, Risueño MC, Leuschner C, Pretzsch H, editors. *Progress in botany*. 84. Cham: Springer; 2022. p. 221–240.
- Roig-Villanova I, Martínez-García JF. Plant responses to vegetation proximity: a whole life avoiding shade. *Front Plant Sci*. 2016;7:236. <https://doi.org/10.3389/fpls.2016.00236>
- Sellaro R, Yanovsky MJ, Casal JJ. Repression of shade-avoidance reactions by sunfleck induction of HY5 expression in *Arabidopsis*. *Plant J*. 2011;68(5):919–928. <https://doi.org/10.1111/j.1365-313X.2011.04745.x>
- Sessa G, Carabelli M, Sassi M, Ciolfi A, Possenti M, Mittempergher F, Becker J, Morelli G, Ruberti I. A dynamic balance between gene activation and repression regulates the shade avoidance response in *Arabidopsis*. *Genes Dev*. 2005;19(23):2811–2815. <https://doi.org/10.1101/gad.364005>
- Shi H, Zhong S, Mo X, Liu N, Nezames CD, Deng XW. HFR1 sequesters PIF1 to govern the transcriptional network underlying light-initiated seed germination in *Arabidopsis*. *Plant Cell*. 2013;25(10):3770–3784. <https://doi.org/10.1105/tpc.113.117424>
- Šimura J, Antoniadis I, Široká J, Tarkovská D, Strnad M, Ljung K, Novák O. Plant hormonomics: multiple phytohormone profiling by targeted metabolomics. *Plant Physiol*. 2018;177(2):476–489. <https://doi.org/10.1104/pp.18.00293>
- Smith H. Light quality, photoperception, and plant strategy. *Ann Rev Plant Physiol*. 1982;33(1):481–518. <https://doi.org/10.1146/annurev.pp.33.060182.002405>
- Sorin C, Salla-Martret M, Bou-Torrent J, Roig-Villanova I, Martínez-García JF. ATHB4, a regulator of shade avoidance, modulates hormone response in *Arabidopsis* seedlings. *Plant J*. 2009;59(2):266–277. <https://doi.org/10.1111/j.1365-313X.2009.03866.x>
- Stepanova AN, Robertson-Hoyt J, Yun J, Benavente LM, Xie D-Y, Doležal K, Schlereth A, Jürgens G, Alonso JM. TAA1-mediated auxin biosynthesis is essential for hormone crosstalk and plant development. *Cell*. 2008;133(1):177–191. <https://doi.org/10.1016/j.cell.2008.01.047>
- Strasser B, Sánchez-Lamas M, Yanovsky MJ, Casal JJ, Cerdán PD. *Arabidopsis thaliana* life without phytochromes. *Proc Natl Acad Sci U S A*. 2010;107(10):4776–4781. <https://doi.org/10.1073/pnas.0910446107>
- Suzuki M, Yamazaki C, Mitsui M, Kakei Y, Mitani Y, Nakamura A, Ishii T, Soeno K, Shimada Y. Transcriptional feedback regulation of YUCCA genes in response to auxin levels in *Arabidopsis*. *Plant Cell Rep*. 2015;34(8):1343–1352. <https://doi.org/10.1007/s00299-015-1791-z>
- Takato S, Kakei Y, Mitsui M, Ishida Y, Suzuki M, Yamazaki C, Hayashi K-I, Ishii T, Nakamura A, Soeno K, et al. Auxin signaling through SCFTIR1/AFBs mediates feedback regulation of IAA biosynthesis. *Biosci Biotechnol Biochem*. 2017;81(7):1320–1326. <https://doi.org/10.1080/09168451.2017.1313694>
- Tanaka S-I, Nakamura S, Mochizuki N, Nagatani A. Phytochrome in cotyledons regulates the expression of genes in the hypocotyl through auxin-dependent and -independent pathways. *Plant Cell Physiol*. 2002;43(10):1171–1181. <https://doi.org/10.1093/pcp/pcf133>
- Tao Y, Ferrer J-L, Ljung K, Pojer F, Hong F, Long JA, Li L, Moreno JE, Bowman ME, Ivans LJ, et al. Rapid synthesis of auxin via a new tryptophan-dependent pathway is required for shade avoidance in plants. *Cell*. 2008;133(1):164–176. <https://doi.org/10.1016/j.cell.2008.01.049>
- Toledo-Ortiz G, Huq E, Rodriguez-Concepcion M. Direct regulation of phytoene synthase gene expression carotenoid biosynthesis by phytochrome-interacting factors. *Proc Natl Acad Sci USA*. 2010;107(25):11626–11631.
- Toledo-Ortiz G, Johansson H, Lee KP, Bou-Torrent J, Stewart K, Steel G, Rodríguez-Concepción M, Halliday KJ. The HY5-PIF regulatory module coordinates light and temperature control of photosynthetic gene transcription. *PLoS Genet*. 2014;10(6):e1004416. <https://doi.org/10.1371/journal.pgen.1004416>
- van Gelderen K, Kang C, Paalman R, Keuskamp D, Hayes S, Pierik R. Far-red light detection in the shoot regulates lateral root development through the HY5 transcription factor. *Plant Cell*. 2018;30(1):101–116. <https://doi.org/10.1105/tpc.17.00771>
- Xie Y, Liu Y, Wang H, Ma X, Wang B, Wu G, Wang H. Phytochrome-interacting factors directly suppress MIR156 expression to enhance shade-avoidance syndrome in *Arabidopsis*. *Nat Commun*. 2017;8(1):348. <https://doi.org/10.1038/s41467-017-00404-y>
- Yang C, Xie F, Jiang Y, Li Z, Huang X, Li L. Phytochrome A negatively regulates the shade avoidance response by increasing auxin/

- indole acidic acid protein stability. *Dev Cell*. 2018;44(1):29–41.e4. <https://doi.org/10.1016/j.devcel.2017.11.017>
- Yanovsky MJ, Casal JJ, Whitelam GC. Phytochrome A, phytochrome B and HY4 are involved in hypocotyl growth responses to natural radiation in *Arabidopsis*: weak de-etiolation of the phyA mutant under dense canopies. *Plant Cell Environ*. 1995;18(7):788–794. <https://doi.org/10.1111/j.1365-3040.1995.tb00582.x>
- Zhang X, Huai J, Shang F, Xu G, Tang W, Jing Y, Lin R. A PIF1/PIF3-HY5-BBX23 transcription factor cascade affects photomorphogenesis. *Plant Physiol*. 2017;174(4):2487–2500. <https://doi.org/10.1104/pp.17.00418>
- Zhang S, Li C, Zhou Y, Wang X, Li H, Feng Z, Chen H, Qin G, Jin D, Terzaghi W, et al. TANDEM ZINC-FINGER/PLUS3 is a key component of phytochrome A signaling. *Plant Cell*. 2018;30(4):835–852. <https://doi.org/10.1105/tpc.17.00677>
- Zhang R, Yang C, Jiang Y, Li L. A PIF7-CONSTANS-centered molecular regulatory network underlying shade-accelerated flowering. *Mol Plant*. 2019;12(12):1587–1597. <https://doi.org/10.1016/j.molp.2019.09.007>
- Zheng Z, Guo Y, Novák O, Chen W, Ljung K, Noel JP, Chory J. Local auxin metabolism regulates environment-induced hypocotyl elongation. *Nat Plants*. 2016;2(4):16025. <https://doi.org/10.1038/nplants.2016.25>